Molecular differentiation in sympatry despite morphological stasis: deep-sea *Atlantoserolis* Wägele, 1994 and *Glabroserolis* Menzies, 1962 from the south-west Atlantic (Crustacea: Isopoda: Serolidae)

ANGELIKA BRANDT[1]*, SASKIA BRIX[2], CHRISTOPH HELD[3] and TERUE CRISTINA KIHARA[4]

[1]*Zoological Institute and Zoological Museum, Biocenter Grindel, University of Hamburg, Martin-Luther-King-Platz 3, 20146 Hamburg, Germany*
[2]*Senckenberg am Meer, German Centre for Marine Biodiversity Research (DZMB), c/o Biocenter Grindel, Martin-Luther-King-Platz 3, D-20146 Hamburg, Germany*
[3]*Alfred Wegener Institute Helmholtz Centre for Polar and Marine Research, Am Alten Hafen 26, D-27568 Bremerhaven, Germany*
[4]*Senckenberg am Meer, German Centre for Marine Biodiversity Research (DZMB), Südstrand 44, D-26382 Wilhelmshaven, Germany*

Received 10 January 2014; revised 23 May 2014; accepted for publication 4 June 2014

During DIVA-3, the third expedition of the DIVA project (Latitudinal gradients of deep-sea biodiversity in the Atlantic Ocean), 45 specimens of Serolidae were obtained from the Argentine Basin, at a depth of about 4600 m. These were a new species of *Glabroserolis* and *Atlantoserolis vemae* (Menzies, 1962). Besides the description of ***Glabroserolis occidentalis* sp. nov.**, *Glabroserolis specialis* Menzies, 1962 is redescribed on the basis of the type material. *Atlantoserolis vemae* is redescribed using the type material, North Atlantic specimens, and the new South Atlantic material. Morphological differences between specimens of *A. vemae* from the North and South Atlantic could not be identified. The molecular data suggest that *A. vemae* from the Argentine Basin comprises two deeply divergent clades, which may represent reproductively isolated, sympatric species.

doi: 10.1111/zoj.12178

ADDITIONAL KEYWORDS: *Atlantoserolis menziesi* – Crustacea – deep sea – ***Glabroserolis occidentalis* sp. nov.** – *Glabroserolis specialis* – Isopoda – molecular genetics – Serolidae – systematics – zoogeography.

INTRODUCTION

Within the suborder Sphaeromatidea Wägele, 1989, the Serolidae Dana, 1853 currently comprises 109 species from 22 genera (Poore & Bruce, 2012). Serolidae were first investigated from Subantarctic and Antarctic localities of the South Atlantic Ocean by Sheppard (1933), on the basis of the genus *Serolis* Leach, 1818. Since then, Serolidae have been considered to occur mainly in the southern hemisphere, being particularly rich in species in the Southern Ocean, Australia, and New Zealand (Harrison & Poore, 1984; Poore 1985, 1987, 1990; Poore & Brandt, 1997; Brandt, 2009; Bruce, 2009; Poore & Storey, 2009; Storey & Poore, 2009). Bruce (2009) noted that only five species are known from the northern hemisphere. Two of these are the deep-sea species: *Atlantoserolis vemae* (Menzies, 1962) and *Atlantoserolis agassizi* (George, 1986). Today, Serolidae are known also from Chile and along the eastern coast of South and North America, up to North Carolina

*Corresponding author. E-mail: abrandt@uni-hamburg.de

(Fig. 1), off South Africa, and Madagascar, as well as in New Zealand (*Brucerolis* Poore & Storey, 2009), and the Coral Sea of Australia (e.g. Poore & Brandt, 1997).

It has been assumed that the deep-sea species are evolutionarily derived from shallow-water ancestors, as most of the deep-sea species have vestigial eyes or lack eyes completely (Brandt, 1991, 1992), and show three centres of radiation (South America, Antarctic, and Australia) after the break-up of Gondwana (Wägele, 1994). Blind deep-sea serolids occur along the South American coast. From there, northward migration probably took place into the north-western Atlantic, and eastwards into the South Pacific (Wägele, 1994). Held (2000) used molecular phylogenetics in order to understand the biogeography of the Serolidae. His data show that the Antarctic species form a monophyletic group, which probably derived from ancestors in South America.

Atlantoserolis, *Caecoserolis*, and *Glabroserolis* form a monophyletic group (Wägele, 1994), to which Bruce (2009) added *Myopiarolis*. *Atlantoserolis* (Cals, 1982) was first mentioned by Cals (1982), but without designation of the type species. Brandt (1991) used the name, and Wägele (1994) stated that the erection of the genus was justified and designated *A. vemae* as the type species. The genus comprises four species, *A. vemae*, *A. agassizi*, *Atlantoserolis menziesi* (Hessler, 1970), and *Atlantoserolis venusta* (Moreira, 1977), and can be distinguished from the other deep-sea genera by having four pairs of separate coxae and a reduced uropod encased in the margin of the pleotelson (Cals, 1982; Poore, 1985). *Glabroserolis* Menzies 1962 has uniramous uropods and no separate coxae, broad antennae and a quadrate maxilliped palp article 2 (Menzies, 1962). Poore (1985) questions the validity of the genus, as none of the characters listed above is unique. Until now, *Glabroserolis* was monotypic and occurred in the Cape Basin off South Africa. Species of *Atlantoserolis* were sampled along the South American coast and North America (Fig. 1, map of the Atlantic Ocean).

Biodiversity within the Serolidae may be underestimated. On the one hand, cryptic species were revealed within the *Ceratoserolis trilobitoides* (Eights, 1833) complex (Held, 2003; Leese & Held, 2008), and Leese *et al*. (2008) found indications for very limited gene flow between populations of *Serolis paradoxa* (Fabricius, 1775). On the other hand, long-distance dispersal (island hopping) via rafting has been documented for *Septemserolis septemcarinata* (Miers, 1881) (Leese, Agrawal & Held, 2010). Recently, Wetzer, Pérez-Losada & Bruce (2013) investigated other species of the Serolidae genetically in order to resolve the phylogenetic relationships of the Sphaeromatidea, but did not include *Atlantoserolis* and *Glabroserolis*.

The bathymetric distribution ranges between shallow waters of 1 m depth for *Leptoserolis nototropis* (Sheppard, 1933) and abyssal depths of 5500 m for *A. vemae* (Menzies, 1962). Compared with many records of species from shelf and bathyal depths, only seven abyssal Serolidae are known from depths below 3500 m (Table 1). The deepest records are known for species of *Atlantoserolis* and *Glabroserolis* (the zoogeographic distribution is illustrated in Fig. 1).

Compared with the deep sea of the northern hemisphere (Sanders & Hessler, 1969; Grassle & Maciolek, 1992; Rex *et al*., 1993; Vincx *et al*., 1994), studies about the deep-sea benthos of the western South Atlantic are rare (e.g. Rex *et al*., 2005a, b). Data on the distribution of isopods from the East Atlantic are published from the DIVA-1 and -2 expeditions with RV *Meteor*, but not a single specimen of Serolidae was found (Fig. 1; Brandt *et al*., 2005; Kröncke, Reiss & Türkay, 2013; source for unpublished data and individual count of isopod families from DIVA-2 extracted from the Deutsche Zentrum für Marine Biodiversitätsforschung, DZMB, database and Nils Brenke, pers. comm.).

Isopoda are known to be highly diverse in the Argentine Basin, even higher than in the Brazilian Basin (Rex *et al*., 1993), and south of the Argentine Basin diversity further increases (Brandt *et al*., 2007), whereas for other taxa like gastropods and bivalves a 'negative' latitudinal gradient with decreasing numbers of species seem to be present, similar to that in the northern hemisphere. Recently new material of *Atlantoserolis* and *Glabroserolis* has been retrieved from abyssal depths of the Argentine Basin. These specimens from a faunistically little known deep-sea basin have been studied, and the species *Glabroserolis occidentalis* sp. nov., *Glabroserolis specialis* Menzies, 1962, and *Atlantoserolis vemae* (Menzies, 1962) are described in the following, in order to improve our understanding of the deep-sea distribution of serolid isopod taxa (Costello, May & Storck, 2013).

MATERIAL AND METHODS

Material studied for comparison

AMNH 12035 *Atlantoserolis vemae* (Menzies, 1962), holotype male.

AMNH 12267 *Atlantoserolis vemae* (Menzies, 1962), paratypes.

USNM 112654 *Atlantoserolis vemae* (Menzies, 1962), 14 individuals from Hessler's (1969) collection, Woods Hole Oceanographic Institute (WHOI) station 70.

USNM 138717 *Atlantoserolis agassizi* (George, 1986), holotype.

USNM 125656 *Atlantoserolis menziesi* Hessler, 1970, holotype male.

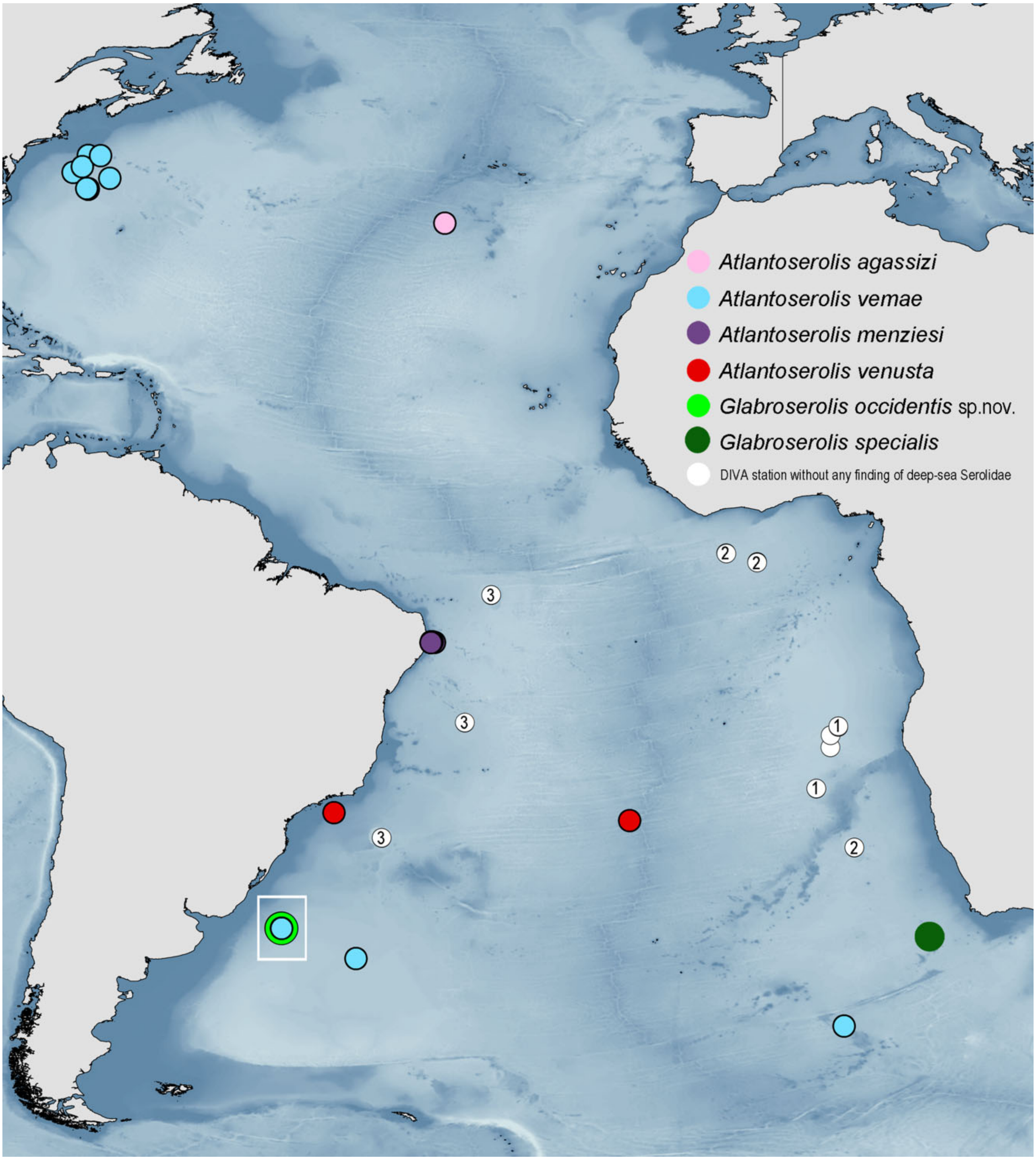

Figure 1. Map of the Atlantic Ocean with all records of *Atlantoserolis* and *Glabroserolis*. The rectangle indicates the stations from which we have obtained molecular data. Each white dot from DIVA-1 (indicated by '1' in the circle) represents one epibenthic sledge (EBS) deployment, from DIVA-2 (indicated by '2' in the circle) two EBS deployments, and from DIVA-3 (indicated by '3' in the circle) three EBS deployments/replicates in the same working area.

Table 1. Abyssal Serolidae occurring at depths greater than 3500 m (compare with Schotte *et al*., 1995, onwards)

Genus	Species	Type locality	Depth (m)
Brucerolis Poore & Storey, 2009	*bromleyana* (Suhm, 1874)	off New Zealand	3612
Acutiserolis Brandt, 1988	*margaretae* (Menzies, 1962C)	S. Atlantic	3813
Brucerolis Poore & Storey, 2009	*maryannae* (Menzies, 1962C)	S. Atlantic	3839
Acutiserolis Brandt, 1988	*neaera* (Beddard, 1884)	Argentine Basin	1097–3731
Glabroserolis Menzies, 1962	*specialis* Menzies, 1962	South Atlantic	4885
Atlantoserolis Wägele, 1994	*vemae* (Menzies, 1962C)	S. Atlantic	4588–5024
Atlantoserolis Wägele, 1994	*agassizi* (George, 1986)	N. Atlantic	3840–3975

USNM 125657 & 12567 *Atlantoserolis menziesi* Hessler, 1970, paratypes female.

AMNH 12124 *Glabroserolis specialis* Menzies, 1962, holotype female.

AMNH 12125 *Glabroserolis specialis* Menzies, 1962, paratypes.

Morphological methods

Drawings were made using a Leica DM 2500 compound microscope with a camera lucida. For the terminology of most important setae types, see Hessler (1970) and Riehl & Brandt (2010). Figures were inked manually and/or digitally according to the method described by Coleman (2003). Manually inked plates were digitalized using Adobe PHOTOSHOP CS5. Holotypes were used for habitus drawings. Where available, appendages were dissected from paratypes. Photographs were taken with an Olympus compound microscope (SZX16 OG88361). Staples were assembled using Helicon Fokus (http://www.heliconsoft.com), manipulated and assembled as plates with Adobe PHOTOSHOP CS5.

SEM: handling of specimens used for pictures

In total, eight *Atlantoserolis* specimens sampled during DIVA-3 at station 533 were used for SEM, as indicated in the descriptions below (Figs 7–28). The specimens were cleaned in an ultrasonic bath for 10 seconds and dehydrated in a series of ethanol concentrations, transferred to 100% acetone, and critical-point dried. After drying they were sputter coated with coal. The specimens were photographed using a Leo 1525 scanning microscope. The resulting digital images were manipulated and assembled as plates with Adobe PHOTOSHOP CS5.

Confocal laser scanning microscopy (CLSM)

Two adult specimens of *Atlantoserolis* sampled during DIVA-3 at stations 533 and 534 were used for CLSM, as indicated in the descriptions below. Before dissection, a female and a male from the South and the North Atlantic was stained with Congo red and acid fuchsin, using procedures adapted from Michels & Büntzow (2010). The whole specimens were temporarily mounted onto slides with glycerine, and self-adhesive plastic reinforcement rings were used to support the coverslip (Kihara & Da Rocha, 2009). When required, specimens were dissected in glycerine under a Leica MZ12 stereomicroscope. Dissected parts were mounted on slides using glycerine as the mounting medium, and self-adhesive plastic reinforcement rings of appropriate thickness were mounted between the slide and the coverslip, so that the parts were not compressed. The material was examined using a Leica TCS SPV equipped with a Leica DM5000 B upright microscope and three visible-light lasers (DPSS 10 mW 561 nm; HeNe 10 mW 633 nm; Ar 100 mW 458, 476, 488, and 514 nm), combined with the software LAS AF 2.2.1 (Leica Application Suite, Advanced Fluorescence). Different objectives were used, depending on the size of the material scanned (Table 2). Images were obtained using only 561-nm excitation with an acousto-optic tunable filter (AOTF), ranging between 40 and 80%, and an excitation beam splitter TD 488/561/633. A series of stacks were obtained, collecting overlapping optical sections throughout the whole preparation, with an optimal number of sections chosen according to the software. The acquisition resolution was 2048 × 2048 pixels, and the settings applied for the preparations are given in Table 2. Final images were obtained by maximum projection, and CLSM illustrations were composed and adjusted for contrast and brightness using the software Adobe PHOTOSHOP CS4.

Molecular methods

DNA extraction of freshly preserved specimens was performed as outlined by Brix, Riehl & Leese (2011). Polymerase chain reaction (PCR) was performed using primer pairs HCO2198/LCOI492, dgHCO/LCOI490, dgHCO/dgLCO, or CrustF/HCO2198 for cytochrome *c* oxidase subunit I (*COI*; Folmer *et al*., 1994; Teske *et al*., 2006), 16Sar/16Sbr for *16S* (Palumbi & Benzie, 1991), and 18A1neu/1155R or 18A1neu/1800neu for *18S* (Raupach & Wägele, 2006). Protocols for PCR are listed

Table 2. List of scanned material with information on objectives and confocal laser scanning microscopy (CLSM) settings for *Atlantoserolis vemae* (Menzies, 1962)

Preparation	Objective	Detected emission wavelength (nm)	Electronic zoom	Pinhole aperture (μm)
Habitus, female and male (Figs 17A, B, 19A, B)	PL FLUOTAR 2.5 × 0.07 DRY	573–682	1.0	68.7–75.8
Habitus, female and male North Atlantic specimens (Figs 23A, B, 25A, B)	PL FLUOTAR 2.5 × 0.07 DRY	573–775	1.0	70.4
Oral region, female and male (Figs 18A, 20A, B)	HCX PL APO CS 10.0 × 0.40 DRY UV	578–643	1.0	28.2–34.8
Mouth parts, male (Fig. 20D–G)	HCX PL APO CS 10.0 × 0.40 DRY UV and HCX APO U-V-I 40.0×/0.75 DRY UV	575–775	1.0–2.0	48.1–53.0
Pereopod I, female and male (Figs 21B, C, 21A, B)	HCX PL APO CS 20.0×/0.70 IMM UV	573–680	1.0	58.5–60.7
Pereopod I, female and male North Atlantic specimens (Figs 24A, 26A)	HCX PL APO CS 10.0 × 0.40 DRY UV	573–731	1.0	24.8–69.9
Pereopod I detail, female North Atlantic specimen (Fig. 24B)	HCX PL APO CS 20.0×/0.70 IMM UV	573–731	2.5	43.1
Pereopod II, male (Fig. 21C, D)	HCX PL APO CS 10.0 × 0.40 DRY UV	573–641	2.0	59.0
Pereopod II, male North Atlantic specimen (Fig. 26B)	HCX PL APO CS 10.0 × 0.40 DRY UV	578–643	1.5	39.7
Pleopod II, male (Fig. 21E, E′, E″)	HCX APO U-V-I 40.0×/0.75 DRY UV	575–775	1.0	48.3

in Table 4. An aliquot of 2–4 μL of undiluted DNA extraction was stored together with the voucher specimen at −20 °C. Purified PCR products were sent for sequencing to QIAGEN (Germany). All Sanger sequence reads were assembled by name into contigs representing 24 specimens and three genes (Table 3) in CODONCODE ALIGNER 4.1.1. All contigs were aligned and visually inspected for quality, and only double-stranded contigs were considered for final analysis. For every position in the three alignments that was found to differ among the specimens, the raw reads were inspected for plausibility. Segregating nucleotides were retained if both reads supported the novel character states, otherwise the respective International Union of Pure and Applied Chemistry (IUPAC) code was assigned. The three resulting alignments (*16S* with 20, *COI* with 18, *18S* with 19 specimens) were trimmed to minimize trailing gaps and to ensure the correct reading frame for *COI*. For the visualization of the barcoding gap analysis, pairwise Kimura two-parameter distance (K2P) matrices were calculated in MESQUITE 2.75 (Maddison & Maddison, 2011) and sorted into bin widths of 0.001 for the mitochondrial genes and 0.0001 for the nuclear *18S* gene in MS EXCEL. Networks of haplotypes were constructed using HAPLOVIEWER (http://www.cibiv.at/~greg/haploviewer), based on an unrooted phylogenetic tree calculated in GENEIOUS 6.1.6 (http://www.geneious.com/), using the HKY85 substitution model with four rate categories and estimating the transition/transversion ratio (*Ti*/*T*v), the proportion of invariable sites and the distribution parameter (γ) from the input alignments. Our preference for low-complexity models of molecular substitution reflects the fact that our aim was reliable estimation of pairwise genetic distances of recently diverged specimens for the purpose of species delimitation, rather than constructing a phylogeny (Lefebure *et al.,* 2006). Simpler models have smaller variance and need less data to converge at meaningful results than more complex, parameter-rich models (Posada & Buckley, 2004). New sequences were deposited in GenBank (accession numbers 16S: KJ950643-KJ950663; 18S: KJ950664-KJ950682; CO1: KJ950683-KJ950701).

Abbrevations

A1, antennula; A2, antenna; AMNH, American Museum of Natural History; Ip, incisior process; lm, lacinia

Table 3. List of voucher specimens used for the genetic study, located at the Zoological Museum Hamburg (ZMH) or the German Centre of Marine Biodiversity Research (DZMB HH), and all available information

Expedition	Deep-sea basin/station	Taxon (type status)	Seqs	GenBank accession number(s)	DZMB-HH and/or ZMH catalogue number	Expedition identification number	Size (mm)	Sex/stage
DIVA-3	ARB/532	*Atlantoserolis vemae*	*COI* *18S*	KJ950683 KJ950664	DZMB-HH 13419 ZMH K–44086	KJ101	< 3	Female
DIVA-3	ARB/534	*Atlantoserolis vemae*	*16S*	KJ950660	DZMB-HH 11390 ZMH K-44088	KJ102	5	Female
DIVA-3	ARB/534	*Atlantoserolis vemae*	*COI* *16S* *18S*	KJ950684 KJ950650 KJ950665	DZMB-HH 14807 ZMH K-44088	KJ103	2.2	Juvenile
DIVA-3	ARB/534	*Atlantoserolis vemae* (figures)	*COI* *16S* *18S*	KJ950685 KJ950651 KJ950666	DZMB-HH 14808 ZMH K-44088	KJ104	4.5	Male
DIVA-3	ARB/534	*Atlantoserolis vemae*	*COI* *16S* *18S*	KJ950686 KJ950652 KJ950667	DZMB-HH 14809 ZMH K-44088	KJ105	4.8	Male
DIVA-3	ARB/534	*Atlantoserolis vemae*	*COI* *16S* *18S*	KJ950699 KJ950644 KJ950680	DZMB-HH 14810 ZMH K-44088	KJ106	2.1	Juvenile
DIVA-3	ARB/534	*Atlantoserolis vemae*	*COI* *16S* *18S*	KJ950688 KJ950654 KJ950669	DZMB-HH 14811 ZMH K-44088	KJ107		Female
DIVA-3	ARB/534	*Atlantoserolis vemae* (figures)	*COI* *16S* *18S*	KJ950689 KJ950655 KJ950670	DZMB-HH 14812 ZMH K-44088	KJ108	4	Female
DIVA-3	ARB/534	*Atlantoserolis vemae*	*16S*	KJ950659	DZMB-HH 14813 ZMH K-44088	KJ109	2.9	Juvenile
DIVA-3	ARB/534	*Atlantoserolis vemae*	*COI* *16S* *18S*	KJ950690 KJ950662 KJ950671	DZMB-HH 14814 ZMH K-44088	KJ110	2.7	Juvenile
DIVA-3	ARB/534	*Atlantoserolis vemae*	*16S*	KJ950653	DZMB-HH 14815 ZMH K-44088	KJ111	< 2	Juvenile
DIVA-3	ARB/534	*Atlantoserolis vemae* (figures)	*COI* *16S* *18S*	KJ950691 KJ950661 KJ950672	DZMB-HH 14816 ZMH K-44088	KJ112	4	Female
DIVA-3	ARB/534	*Atlantoserolis vemae*	*COI* *16S* *18S*	KJ950692 KJ950648 KJ950673	DZMB-HH 14817 ZMH K-44088	KJ113	2	Juvenile
DIVA-3	ARB/534	*Atlantoserolis vemae*	*COI* *16S* *18S*	KJ950693 KJ950649 KJ950674	DZMB-HH 14818 ZMH K-44088	KJ114	4	Female
DIVA-3	ARB/534	*Atlantoserolis vemae*	*18S* *COI*	KJ950677 KJ950696	DZMB-HH 14819 ZMH K-44088	KJ115	4	Male
DIVA-3	ARB/534	*Atlantoserolis vemae*	*COI* *16S* *18S*	KJ950697 KJ950643 KJ950678	DZMB-HH 14820 ZMH K-44088	KJ116	2.7	Juvenile
DIVA-3	ARB/534	*Atlantoserolis vemae*	*COI* *16S* *18S*	KJ950698 KJ950645 KJ950679	DZMB-HH 14821 ZMH K-44088	KJ117	3.2	Juvenile
DIVA-3	ARB/534	*Atlantoserolis vemae*	*16S*	KJ950657	DZMB-HH 14822 ZMH K-44088	KJ118	2.8	Juvenile
DIVA-3	ARB/534	*Glabroserolis occidentalis* (holotype)	*COI* *16S* *18S*	KJ950701 KJ950663 KJ950682	DZMB-HH 14823 ZMH K-44083	KJ119	4	Female
DIVA-3	ARB/534	*Atlantoserolis vemae*	*18S* *COI*	KJ950675 KJ950694	DZMB-HH 14824 ZMH K-44088	KJ120	4.5	Male
DIVA-3	ARB/534	*Atlantoserolis vemae*	*16S*	KJ950646	DZMB-HH 14825 ZMH K-44088	KJ121	3.2	Juvenile
DIVA-3	ARB/534	*Atlantoserolis vemae*	*COI* *16S* *18S*	KJ950700 KJ950647 KJ950681	DZMB-HH 14826 ZMH K-44088	KJ122	4.5	Oov. female
DIVA-3	ARB/534	*Atlantoserolis vemae*	*16S*	KJ950658	DZMB-HH14827 ZMH K-44088	KJ123		
DIVA-3	ARB/534	*Atlantoserolis vemae*	*16S*	KJ950656	DZMB-HH 14828 ZMH K-44088	KJ124		

ARB, Argentine Basin. All other specimens used for species description and comparative specimens are listed in the species descriptions.

Table 4. Main protocols for polymerase chain reaction (PCR) of DIVA-3 extractions for all three markers

PCR mix volumes (μL)	*COI*	*18S*	*16S*
dNTPs	1	1	1
Buffer	6	6	6
ddH_2O (μL)	13.7	13.7	13.7
Primer 1 (10–12 μM)	1	1	1
Primer 2 (10–12 μM)	1	1	1
Template DNA (μL)	3	3	3
Polymerase	0.3	0.3	0.3
Total volume (μL)	25	25	25
PCR protocol			
Preheated lid	Yes	No	Yes
Initial denaturation time (min:sec)	01:00	05:00	01:00
Initial denaturation temperature (°C)	94	94	94
Denaturation time (min:sec)	00:30	01:00	00:30
Denaturation temperature (°C)	94	94	94
Annealing time (min:sec)	00:30	01:00	00:30
Annealing temperature (°C)	47	52	52
Elongation time (min:sec)	01:20	03:20	01:00
Elongation temperature (°C)	72	72	72
Cycle number	40	40	37
Final elongation time (min:sec)	05:00	07:00	05:00

mobilis; lMd, left mandible; mp, molar process; Op, operculum; PI–PVII, pereopods I–VII; Pln 1–3, pleonites 1–3; Plp 1–5, pleopods 1–5; Plt, pleotelson; Prn 1–7, pereonites 1–7; rMd, right mandible; Urp, uropods; USNM, United States National Museum of Natural History, Washington; ZMH, Zoological Museum, Hamburg.

RESULTS

Taxonomy

Sphaeromatidea Wägele, 1989

Serolidae Dana, 1853

The most recent family diagnosis is provided in Brandt & Poore (2003).

Genus *Glabroserolis* Menzies, 1962

Glabroserolis Menzies, 1962: 189–190; – Wägele, 1994: 52; Poore, 1985: 175; Bruce, 2009: 39; Held, 2000: 176.

Type species
Glabroserolis specialis Menzies, 1962.

Diagnosis
Coxal plates not marked off at any pereonal somites. Uropods uniramous.

Glabroserolis specialis Menzies, 1962 (Figs 2, 6).

Glabroserolis specialis Menzies, 1962: 189–190; – Wägele, 1994: 52; Poore, 1985: 175; Bruce, 2009: 39.

Material examined
Holotype: Female, 3.3 mm in length, AMNH 12124, south-east Atlantic at a depth of 4885 m (Menzies, 1962).

Paratypes: AMNH 12125.

Redescription of *Glabroserolis specialis* Menzies, 1962

Holotype: Female (3.3 mm); anterolateral angles of head slightly elongate laterally (Fig. 2); head frontally as wide as mesiolaterally, mediocaudally fused with Prn 1. Eyes absent. Second to sixth Prns with coxal plates not marked off by dorsal sutures, only a faint shallow depression visible (Fig. 2). Posterolateral angles of the coxal plates of Prn 2–6 all reaching slightly further caudally than those of the preceding segments, not increasing in length along Prn 2–6, but with sixth coxal plate longest. Prn 7 partly fused with Prn 6. Pln 1–3 without epimera, surrounded by Prn 6. Pln 1–3 width very slightly increasing, Pln 1–2 length equal. Plt with one semicircularly rounded elevation with two small rounded elevations anterolaterally. Tip of Plt rounded, lateral sides slightly narrowing medially (Fig. 2).

Antennula (A1; Fig. 2) about one-third in width of A2, with three peduncular segments, first one widest and longest, second one almost as long as first one, slightly narrower, and third article narrower and shorter than second. Seven flagellar articles decreasing in length and width towards tip.

A2 (Fig. 2) consisting of five peduncular and nine flagellar articles. First peduncular article very short, quadrangular, covered by antennule in dorsal view; second peduncular article slightly longer than first; third article trapezoidal, slightly wider than second; fourth peduncular article broadest and longest, with several longitudinal rows of groups of simple setae; fifth peduncular article slightly shorter than fourth (0.94) also with groups of setae. All flagellar articles with groups of distolateral simple setae, last article with three setae.

Pereopod I (PI; Fig. 2) stronger than all following pereopods, with long basis, short merus, and ischium and carpus of equal size, propodus broad, subchelate. Basis to merus without any spines or setae, quadrangular carpus with two strong sensory setae. Mediolateral surface of propodus with one long row of setulated sensory setae. Dactylus long and slender, without dactylar claw.

Pereopod II (PII; Fig. 2c) with long and slender basis; ischium 0.5 times length of basis, without setae; merus 0.65 times length of carpus, merus and carpus with three distodorsal, distally slightly setulated setae;

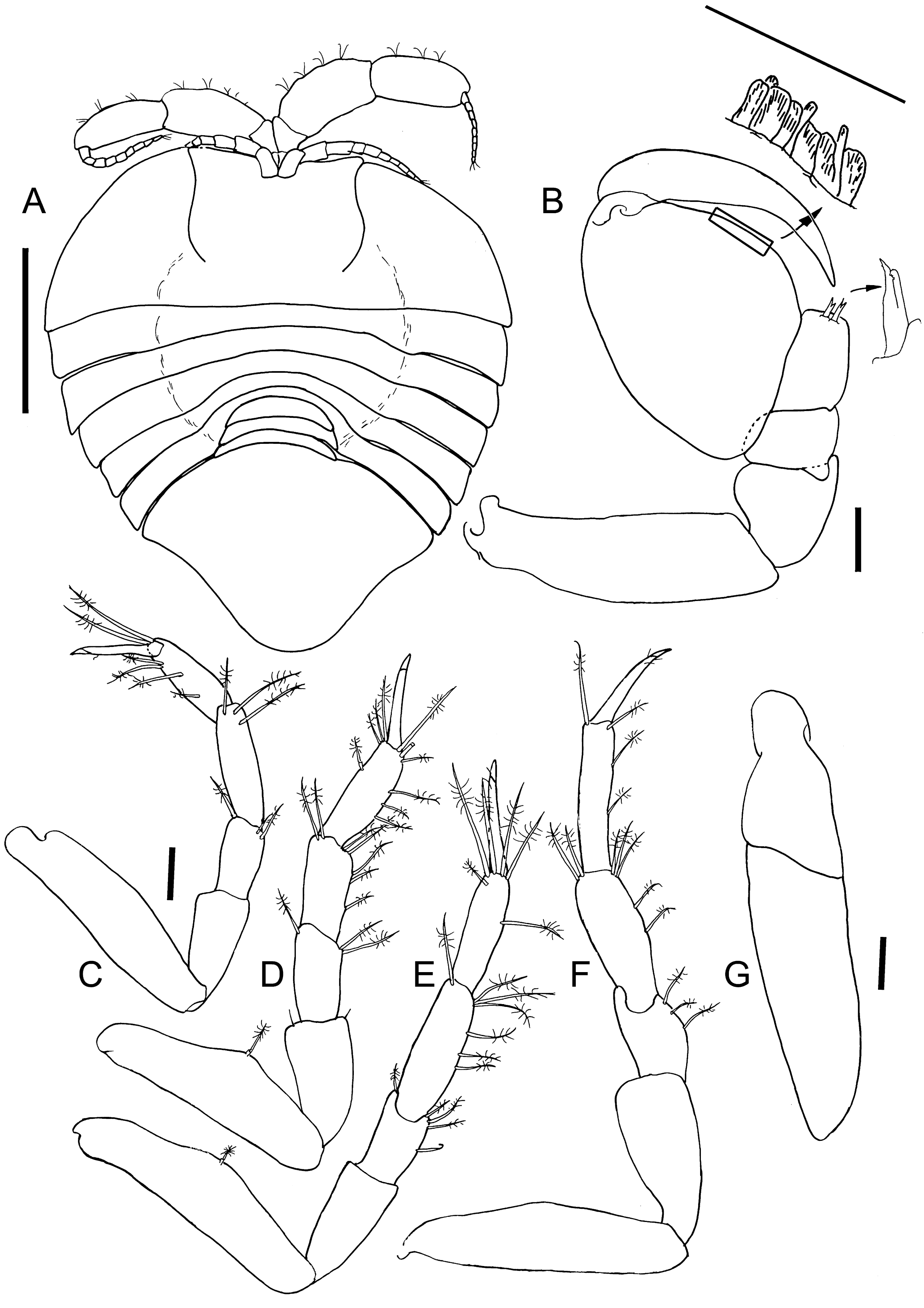

Figure 2. *Glabroserolis specialis* Menzies, 1962. Holotype female in dorsal view (A); pereopods II–IV (B–E); pereopod VI (F); uropod (G). Scale bars: (A) 1 mm; (B–G) 0.1 mm.

propodus 0.7 times length of carpus (twisted), ventrally with four and distodorsally with two long setae similar in shape to those of merus and carpus. Dactylus 0.7 times as long as propodus, with one setule and a short and small claw.

Pereopod III (PIII; Fig. 2d) with long and slender basis, mediodorsally slightly elevated and equipped with a small plumose seta; ischium 0.5 times length of basis, with two simple setae; merus 0.8 times length of carpus, with three distodorsal, distally slightly setulated setae; carpus about as long as merus, with four distal and three ventral setae distally setulated, propodus 1.1 times length of carpus, ventrally with three, dorsally with one, and distally with six long setae of similar shape as those of merus and carpus. Dactylus 0.7 times length of propodus.

Pereopod IV (PIV; Fig. 2e) with long and slender basis, mediodorsally slightly elevated and equipped with a small plumose seta; ischium 0.4 times length of basis, without setae; merus 0.65 times length of carpus, with three distodorsal, distally slightly setulated setae; carpus about as long as merus, with three distal and three ventral setae distally setulated, propodus 0.95 times length of carpus, with one ventral and five distal long setae of varying lengths, and of similar shape as those of merus and carpus. Dactylus almost as long as propodus (0.9 times length of propodus), with one setule.

Pereopod VI (PVI; Fig. 2f) with long and slender basis, mediodorsally slightly elevated, without setae; ischium 0.5 times length of basis, without setae; merus 0.6 times length of carpus, with three ventral, distally slightly setulated setae; carpus 1.35 times as long as merus, with five distal and two additional ventral setae distally setulated, propodus 0.6 times width and 1.0 times length of carpus, with two ventral and two distal long setae of similar shape as those of merus and carpus. Dactylus 0.7 times length of propodus, with three setules.

Pereopod VII (PVII; Fig. 6) absent.

Uropod (Urp; Fig. 2) with elongate sympodite, only one ramus, 2.2 times length of sympodite, distally slightly acuminating, tip rounded.

Remarks
Glabroserolis was monotypic, it could easily be distinguished from other serolids by the diagnostic genus characters. Differences between *G. specialis* and *G. occidentalis* sp. nov. are discussed under the remarks for *G. occidentalis* sp. nov.

GLABROSEROLIS OCCIDENTALIS BRANDT & BRIX **SP. NOV.** (FIGS 3–6)

Material examined
Holotype: Female, 4 mm in length (ZMH-K 44083), station 534 (RV *Meteor*), 16 July 2009, 049°01.54′–049°01.74′W, 36°00.61′–36°00.69′S, depth 4605–4607 m.

Paratypes: Juvenile, 3 mm in length (ZMH K-44084), station 533 (RV *Meteor*), 15 July 2009, 049°01.96′–049°02.12′W, 36°00.20′–36°00.27′S, depth 4602–4606 m.

Distribution
Argentine Basin, only known from type locality.

Etymology
The epithet '*occidentalis*' (from the Latin *occidens*, meaning west) indicates the West Atlantic finding of this new species, in contrast to *G. specialis*, which was first described from the East Atlantic (Fig. 1).

Description of female holotype (Figs 3–6)
Anterolateral angles of head slightly elongate laterally (Fig. 3); head smooth, frontally slightly wider than mediocaudally and caudally, medially slightly narrowing, caudomedially head fused with first Prn. Eyes absent. Prn 2–4 with coxal plates not marked off by dorsal sutures, with only shallow depressions visible. Posterolateral angles of the coxal plates of Prn 2–6 all reaching slightly further caudally than those of the preceding segments, not increasing in length along Prn 2–6, but with sixth coxal plate longest. Prn 7 partly fused with Prn 6. Pln 1–3 without epimera, surrounded by Prn 6. Plns increasing in width, length of all Plns equal (Fig. 3). Plt with one semicircularly rounded elevation, slightly vaulted caudomedially, protruding in lateral view (Fig. 4) with two small rounded elevations anterolaterally. Tip of Plt rounded, lateral sides slightly narrowing medially (Fig. 3). Ventral view with insertion of pereopods, and shape of labrum and PI.

A1 of holotype female (Fig. 3) with three peduncular segments, first one shorter than second, second one slightly longer but narrower than first, third one as long as first. Seven flagellar articles: first flagellar article broadest, second one longest. Last flagellar article with three simple setae.

A2 of holotype female (Fig. 4d) consisting of five peduncular and nine flagellar articles. First peduncular article very short, almost quadrangular. Second peduncular article slightly longer than third, quadrangular, without setae; third article trapezoidal, with nine distal simple setae; fourth peduncular article a little longer (1.1 times) and broader (1.4 times) than fifth, with several longitudinal rows of groups of two or three simple setae; fifth peduncular article also with groups of setae. All nine flagellar articles with groups of between one and three distolateral simple setae; few aesthetascs.

Pereopod I of holotype female (Fig. 5a) stronger than all following pereopods, with long basis, short merus, and ischium and carpus of equal length, propodus broad, subchelate. Basis to merus without any spines or setae, carpus with two strong sensory setae.

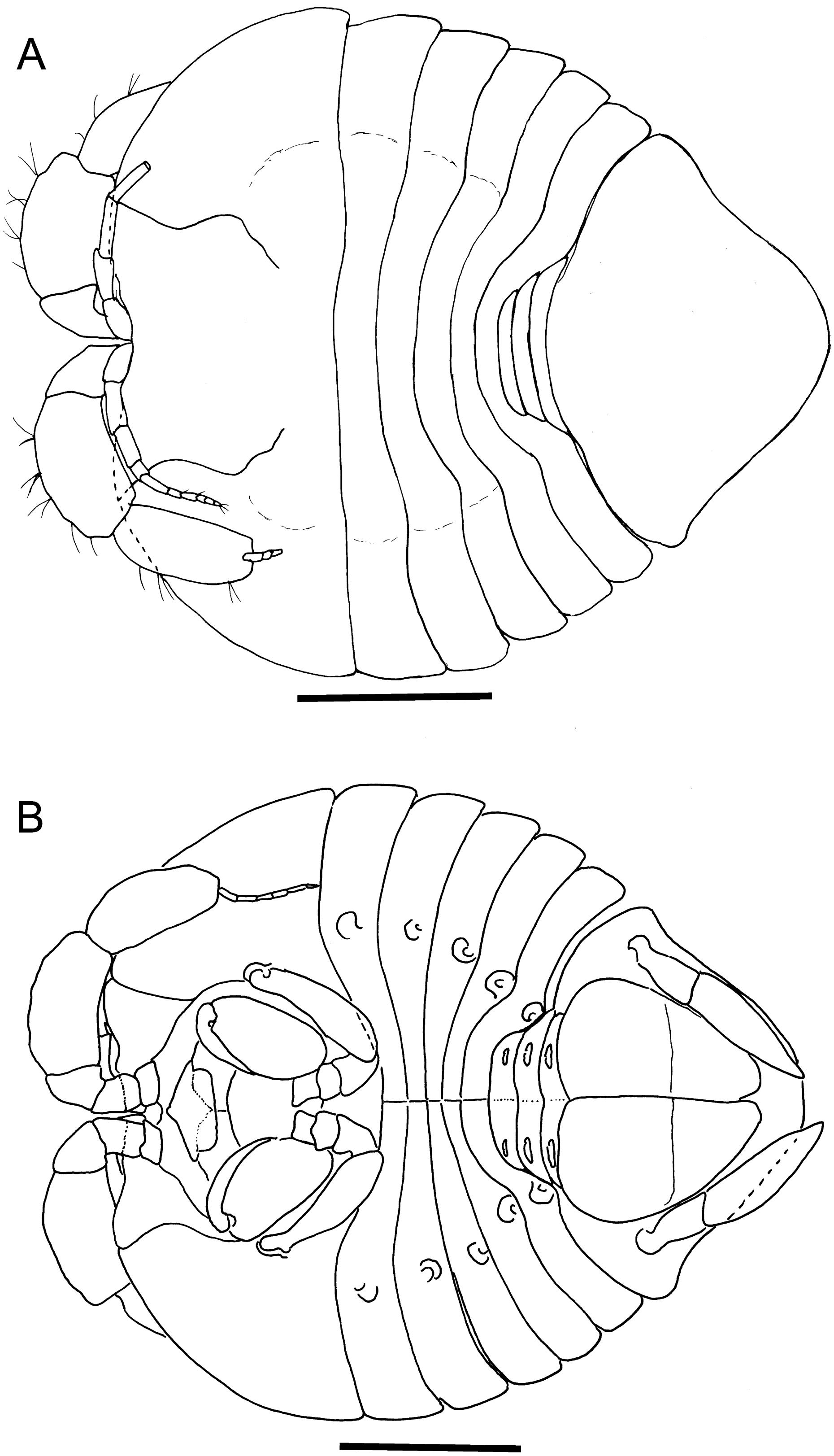

Figure 3. ***Glabroserolis occidentalis*** Brandt & Brix **sp. nov.** Holotype female in dorsal (A) and ventral (B) view. Scale bars: 1 mm; detail of pereopod I 0.1 mm.

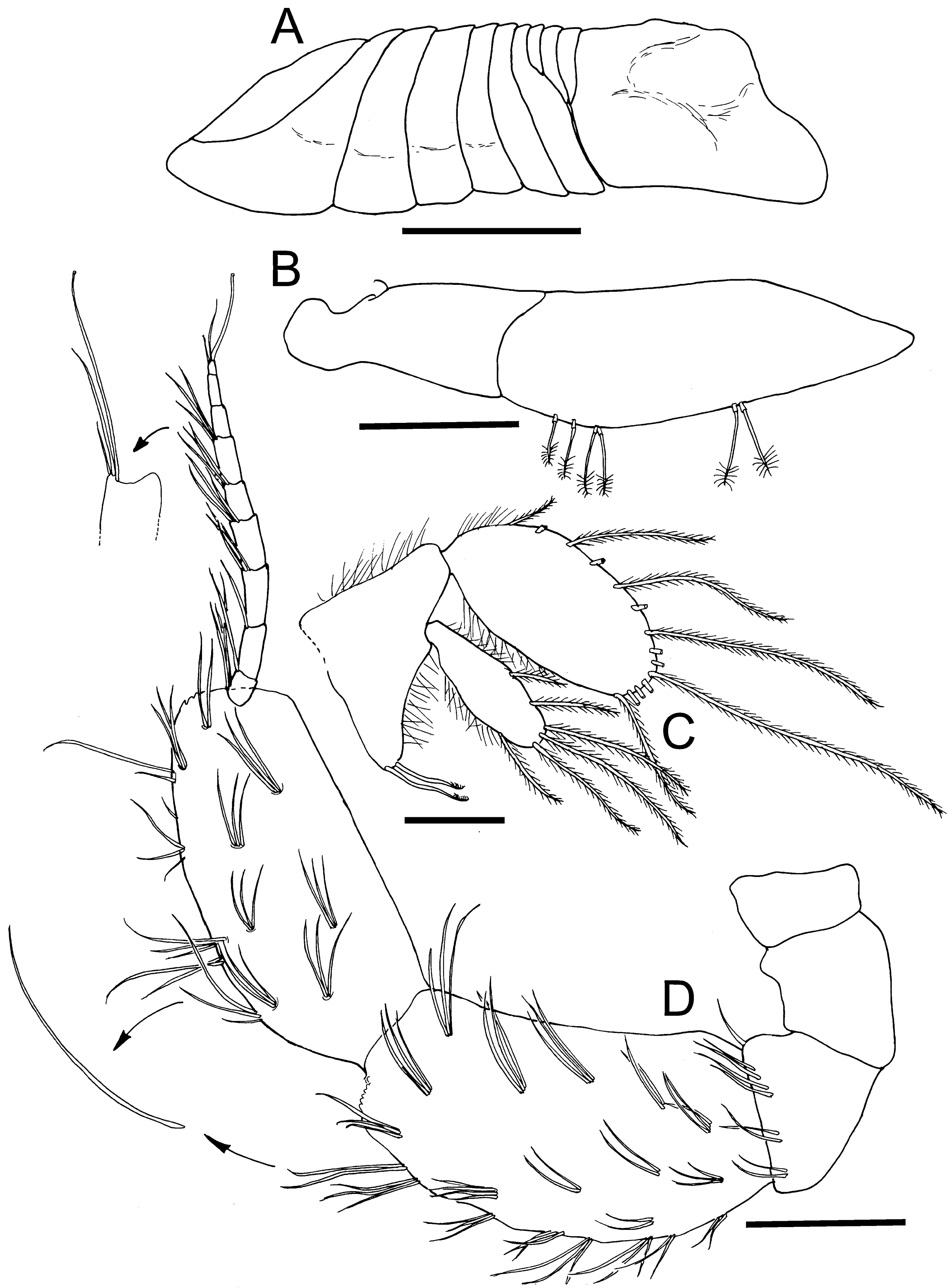

Figure 4. ***Glabroserolis occidentalis*** Brandt & Brix **sp. nov.** Holotype female in lateral view (A); uropod (B); pleopod 1 (C); and antenna (d). Scale bars: (A) 1 mm; (B–D) 0.1 mm.

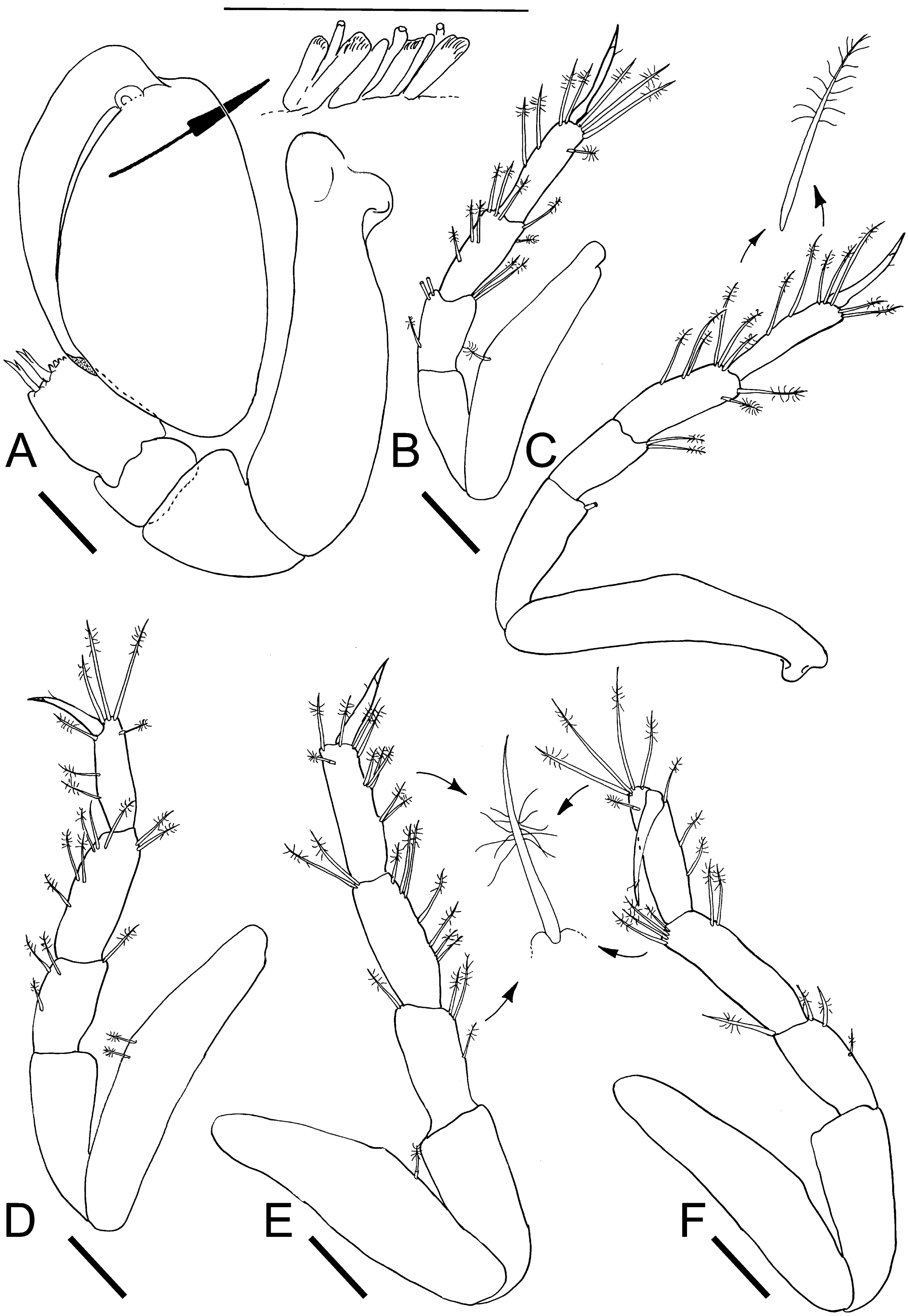

Figure 5. ***Glabroserolis occidentalis*** Brandt & Brix **sp. nov.** Holotype female, pereopods I–VI (A–F). Scale bars: 0.1 mm.

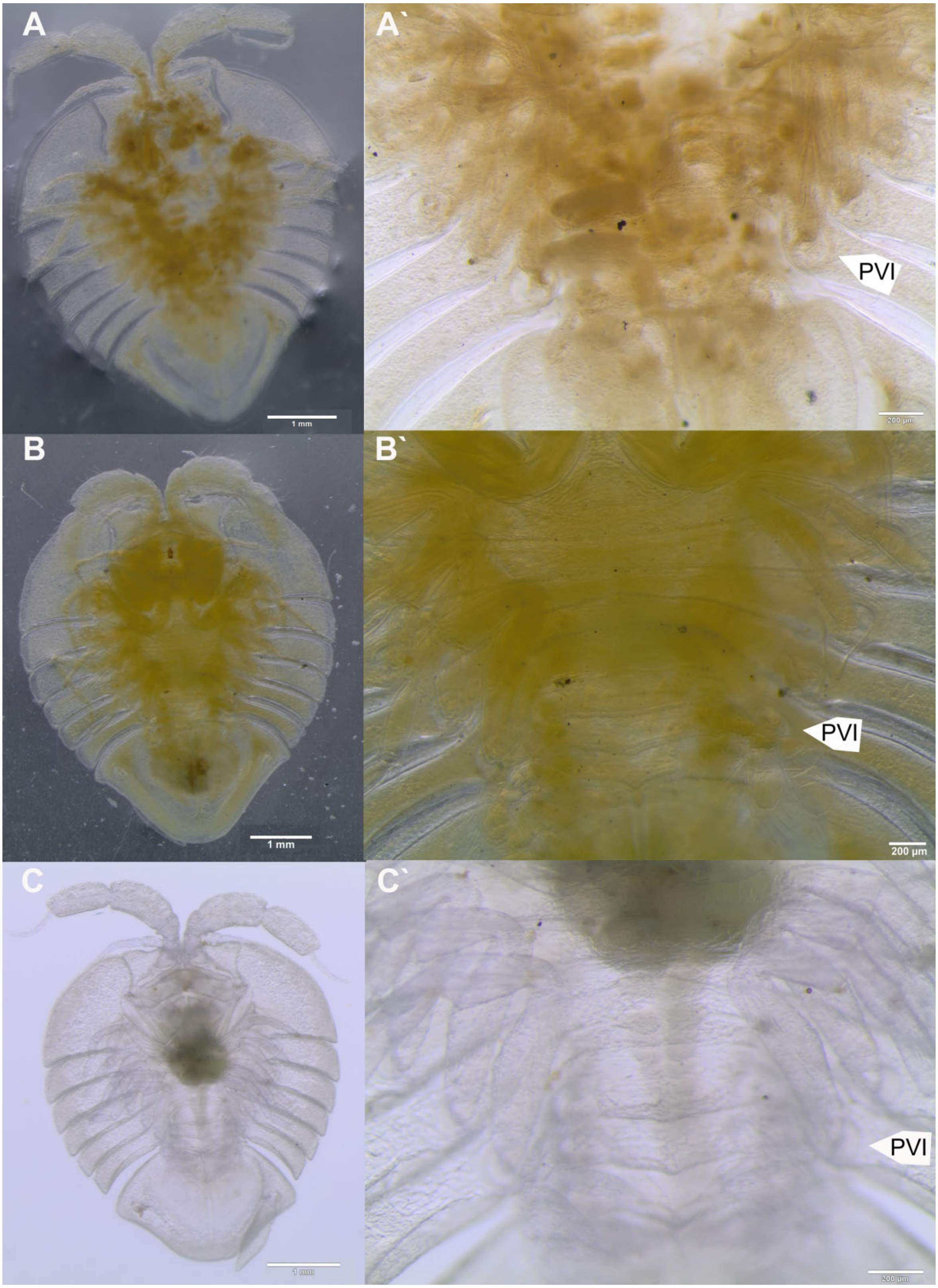

Figure 6. *Glabroserolis specialis* Menzies, 1962, holotype in ventral view (A, A′). ***Glabroserolis occidentalis*** Brandt & Brix **sp. nov.**, holotype in ventral view (B, B′). Paratype of ***Glabroserolis occidentalis*** Brandt & Brix **sp. nov.** in ventral view (C, C′). Arrows point to the insertions of pereopod VI.

Mesiolateral surface of propodus with one long distally split and a row of shorter setulated sensory setae (not illustrated). Dactylus long and slender, without dactylar claw.

Pereopod II (PII) of holotype female (Fig. 5b) with long and slender basis, mediodorsally slightly elevated and equipped with a small plumose seta; ischium 0.4 times length of basis, without setae; merus 0.8 times length of ischium, merus with four distal and one ventral distally slightly setulated setae; Carpus 1.2 times length of merus, with three ventral, one dorsal, and four distal distally setulated setae; propodus 1.1 times length of carpus, ventrally with two, dorsally with one, and distally with five long setae of similar shape as those of merus and carpus; dactylus very slender, 0.9 times as long as propodus, with one setule and a short, small claw.

Pereopod III (PIII) of holotype female (Fig. 5c) with long and slender basis, mediodorsally slightly elevated; ischium 0.5 times length of basis, with one distal seta (broken); merus 0.7 times length of ischium, with two distodorsal, distally slightly setulated setae; carpus 1.1 times as long as merus, with six ventral and two dorsal setae distally setulated; propodus as long as carpus, ventrally with five, distodorsally with two long setae of similar shape as those of merus and carpus; dactylus 0.8 times as long as propodus.

Pereopod IV (PIV) of holotype female (Fig. 5d) with long and slender basis, mediodorsally slightly elevated and equipped with two small plumose setae; ischium 0.4 times length of basis, without setae; merus 0.6 times length of ischium, with three ventral and one distal seta; carpus 1.3 times as long as merus, with six ventral and two distodorsal setae distally setulated; propodus 0.8 times length of carpus, with three ventral, one distodorsal, and three long distal setae, of varying lengths, and of similar shape as those of merus and carpus; dactylus 0.8 times length of propodus, with one setule and one claw.

Pereopod V (PV) of holotype female (Fig. 5e) with long and slender basis, mediodorsally slightly elevated and equipped with one small plumose seta in distodorsal half of article; ischium 0.4 times length of basis, without setae; merus 0.8 times length of ischium, with three ventral and one distal distally setulated seta; carpus 1.2 times as long as merus, with seven ventral and two distodorsal distally setulated setae; propodus as long as carpus, with seven ventral, one dorsal, and two long distal setae, of similar shape as those of merus and carpus; dactylus 0.8 times length of propodus, with one setule and one claw.

Pereopod VI (PVI) of holotype female (Fig. 5f) with long and slender basis, distally slightly elevated, without setae; ischium 0.4 times length of basis, without setae; merus 1.6 times length of ischium, with three ventral and one distal, distally slightly setulated, setae; carpus 1.6 times as long as merus and as long as ischium, with four dorsal and two ventral distally setulated setae, propodus 0.8 times as long and 0.9 times as wide as carpus, with two ventral, one dorsal, and five distal setulated setae of different lengths; dactylus almost as long as propodus, with one setule and one claw.

Pereopod VII (PVII; Fig. 6) absent.

Pleopod 1 of holotype female (Fig. 3c) with long trapezoidal sympodite, bearing two proximomedial setulated setae with setulated tuft (similar to a brush). Endopodite (with six) and exopodite (with 14) with many long plumose setae of varying lengths, endopodite smaller.

Uropod (Urp) of holotype female (Fig. 3b) with elongate sympodite of quadrangular shape; only one ramus 1.8 times as long and 1.5 times as broad as sympodite, with six lateral plumose setae.

Remarks

Glabroserolis occidentalis Brandt & Brix sp. nov. is the second species of the genus. It has been sampled from the Argentine Basin in the West Atlantic. It differs from *G. specialis* Menzies, 1962 in the shape of the Plt, which is smooth in *G. specialis*; however, in *G. occidentalis* it bears a semicircularly rounded elevation, which is pronounced and slightly vaulted caudomedially, as illustrated in Figure 4a. In both species of *Glabroserolis*, PVII is not developed (Fig. 6). Menzies (1962) describes *G. specialis* based on a specimen of 3.3 mm in length, designated as female. We re-examined the holotype and prepared a ventral view (Fig. 6); PVII is missing in *G. specialis* as well as in the new species *G. occidentalis* sp. nov. As we have no males or ovigerous females available, it is impossible to describe the missing pereopod as a synaponorphic character of the two species, as we might have immature females to hand. Future sampling of a male or adult (brooding) female will reveal whether this is a synapomorphic character of *G. specialis* and *G. occidentalis* sp. nov., or whether both Menzies and ourselves had only immature specimens to hand (Fig. 6). The lack of PVII in adult isopods has already been described for some Anthuroidea (Wolff, 1962; Poore, 1984), and for *Stylomesus hexapodus* Brökeland & Brandt, 2004, *Haplomesus corniculatus* Brökeland & Brandt, 2004, *Dendromunna mirabile* Wolff, 1962, *Munella danteci* Bonnier, 1896, and *Lipomera lamellata* Tattersall, 1905.

ATLANTOSEROLIS WÄGELE, 1994

Atlantoserolis Wägele, 1994: 9–10; Poore, 1985: 175; Bruce, 2009: 39; Held, 2000: 176.

Genus diagnosis (modified after Wägele, 1994)

Body oval, about as wide as long, flattened and without dorsal ornamentation, eyes absent; pereonites with all segments indicated by entire suture lines, coxal plates large, suture lines between coxal plates 2–5 and tergites dorsally visible, distal margins truncate; last coxal plates framing the narrow epimera of Pln 2 and 3; Plt distally rounded or tapering to apex; Plt 1.15 times as wide as long; PI palm setae comprising one long row of distally bifid sensory setae and one short row of setulated sensory setae, male PII with palm roughly straight at oval propodus; palp of maxilliped of three articles; uropod with one minute ramus and one ramus longer than sympod.

Remarks
As most of the mouthparts of this genus were unknown, a redescription of the type species is valuable and is presented herewith on the basis of Menzies's type material from the AMNH as well as new material collected during the DIVA-3 expedition.

Type species
Serolis (*Serolis*) *vemae* Menzies, 1962.

Type locality
South Atlantic, Argentine Basin, 4588–5024 m depth.

Composition
Atlantoserolis vemae (Menzies, 1962), *A. agassizi* (George, 1986), *A. menziesi* (Hessler, 1970), *A. venusta* (Moreira, 1977).

ATLANTOSEROLIS VEMAE (MENZIES, 1962) (FIGS 7–27)

Serolis Menzies, 1962: 188–189; *Atlantoserolis* Wägele, 1994: 9–10; Poore, 1985: 175; Bruce, 2009: 39; Held, 2000: 176.

Material examined
Holotype: Male, 4.1 mm in length, AMNH 12035, *A. vemae* (Menzies, 1962), depths of 4588 and 5024 m in the South Atlantic (Menzies, 1962).

Paratypes: Female, 6.0 mm in length, AMNH 12267.

Additional material: Fourteen juveniles of 2.0–3.2 mm in length, 11 males of 4–5 mm in length and 15 females of 4–6 mm in length from station 532 (one female) (ZMH K-44086), 049°00.75′–049°00.89′W, 35°59.16′S–35°59.24′S, depth 4605 m; station 533 (four females, three males, two juveniles) (ZMH K-44087), 15 July 2009, 049°01.96′–049°02.12′W, 36°00.20′–36°00.27′S, depth 4602–4606 m; station 534 (nine females, eight males, 12 juveniles) (ZMH K-44088), 16 July 2009, 049°01.54′–049°01.74′W, 36° 00.61′–36°00.69′S, depth 4605–4607 m.

USNM 112654, *A. vemae* (Menzies, 1962), redescribed by Hessler based on 14 individuals from Hessler's (1969) collection, W.H.O.I. station 70, depth 2862–4749 m in the North Atlantic (Hessler, 1967). The body size of *A. vemae* from Hessler's material varies between 2 mm (stage-1 early manca) and 6.5 mm (copulatory male).

Atlantoserolis vemae (Menzies, 1962) (Figs 7–27)
Figure 6 shows photographs of three specimens of *A. vemae* that are almost the same size: A, type material that was sampled and illustrated by Menzies (1962); B, a specimen of *A. vemae* sampled during the DIVA-3 expedition from station 534 in the Argentine Basin of the South Atlantic (Figs 1, 6b, 10–12); and C, a picture of *A. vemae* from the North Atlantic sampled by Hessler and redescribed as *A. vemae*. The image shows that these specimens look more opaque, because of a thicker cuticle.

Redescription of male holotype (AMNH 12035)
Greatest width of body (between tips of coxae 2; Figs 8, 10, 11, 15, 16, 18, 20, 23, 24, 26) 0.8 times body length (rostrum to end of Plt). Head with broad diverging anterolateral lobes lateral to bases of antennae, almost straight frontally. Eyes and eye sockets absent. Prn 1 with anterolateral margin continuously convex; posterolateral corner not overlapping coax 2, smooth. Prn 2–4 articulating, with coxal plates marked off by dorsal sutures; Prn 5 also with coxal plate, but placed more medially; Prn 5–7 free, medially shorter than Prn 2–4, Prn 5 laterally as broad as Prn 2–4, Prn 6 slightly shorter. Prn 7 without coxal plates. Posterolateral angles of coxal plates 2–6 protruding posterolaterally, coxal plates forming a nearly continuous margin. Last coxal plates framing the narrow epimera of Pln 2 and 3. Plt distally rounded or tapering to apex, Plt 1.15 as wide as long. Ventral coxal plates 2–5 meeting, swollen, and sculptured in midline; sternites 5–7 fused and visible; ventral coxal plates 6 and 7 separated. Pln 1 only visible ventrally. Dorsally, Pln 2 and 3 with narrow epimera of comparable length and width, both reaching 30% of Plt length.

Plt slightly less than a third of length of body, 0.8 times as long as wide, lateral margins slightly rounded, posterior margin acuminating into tip; with obscure mid-dorsal ridge, and almost triangular elevation mediofrontally. Uropods are inserted ventrolaterally at one-third of length.

Antennula (A1; Figs 10, 12, 15, 16, 18, 20) with peduncular article 2 slightly narrower but 1.3 times longer than article 1, article 3 0.9 times shorter than second; flagellum of eight articles; flagellar article 1 longest, slightly less than half length of last peduncle article, with three plumose setae, proximal four

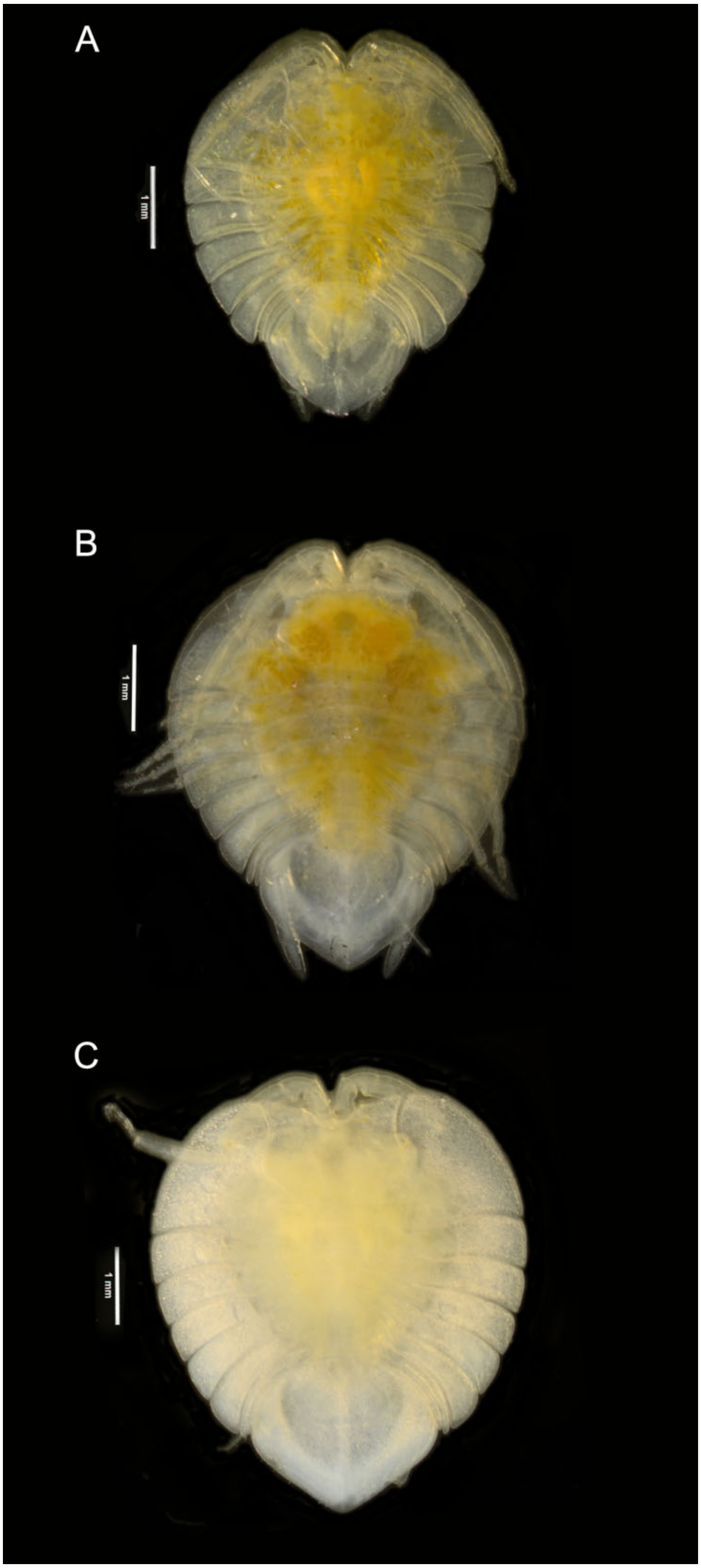

Figure 7. Comparison of three adult male *Atlantoserolis vemae* specimens from three different locations using a compound microscope: A, holotype *A. vemae* AMNH 12035; B, *A. vemae* DZMB HH 14808 from DIVA-3; C, *Atlantoserolis* cf. *vemae* from Woods Hole Oceanographic Institute station 70, sampled by Hessler in the 1960s in the North Atlantic Ocean.

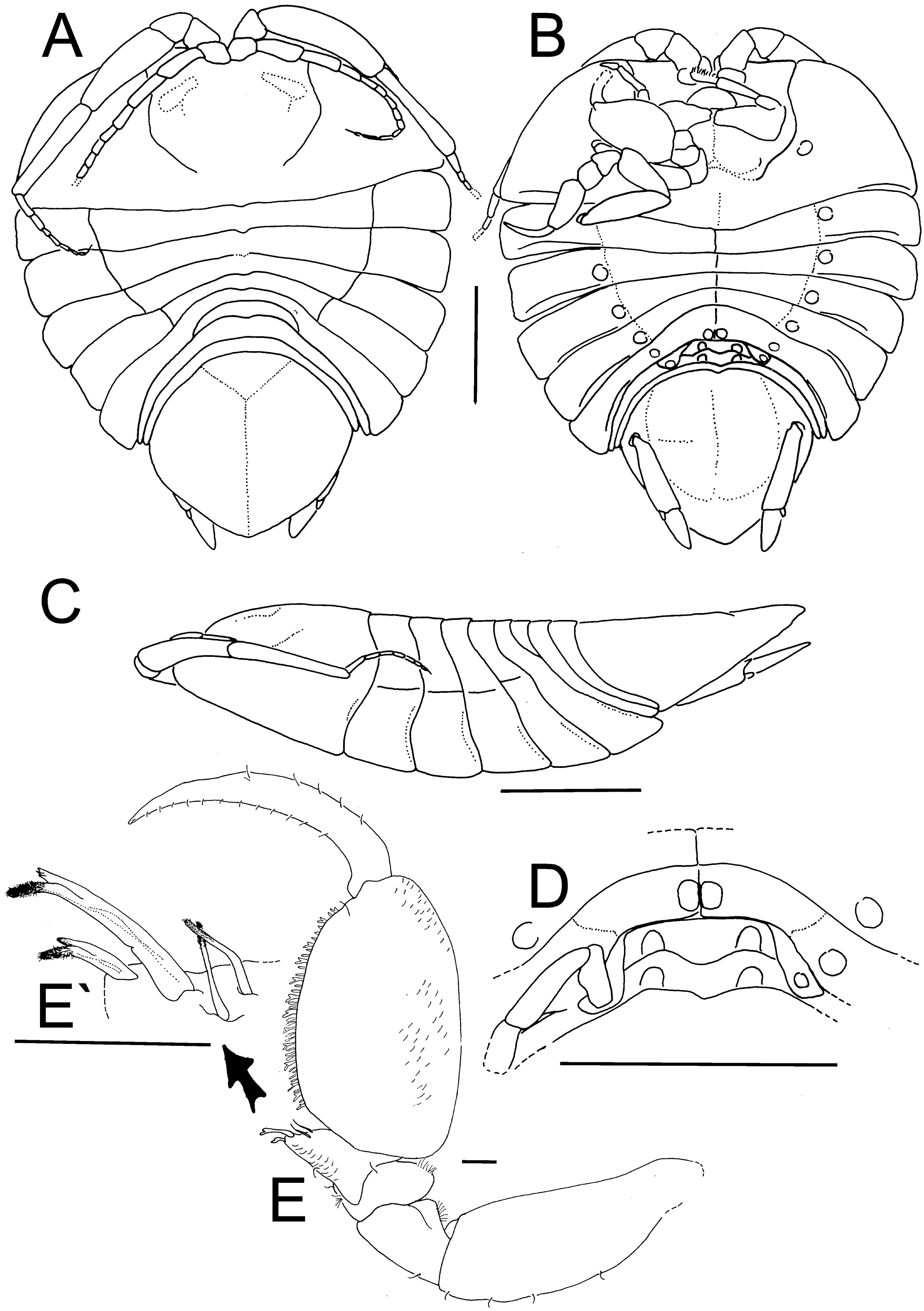

Figure 8. *Atlantoserolis vemae* Menzies, 1962, AMNH 12035, holotype male in dorsal (A) and ventral (B) views, lateral view (C), detailed ventral view (D) and pereopod I (E, E′). Scale bars: (A–D) 1 mm; (E, E′) 0.1 mm.

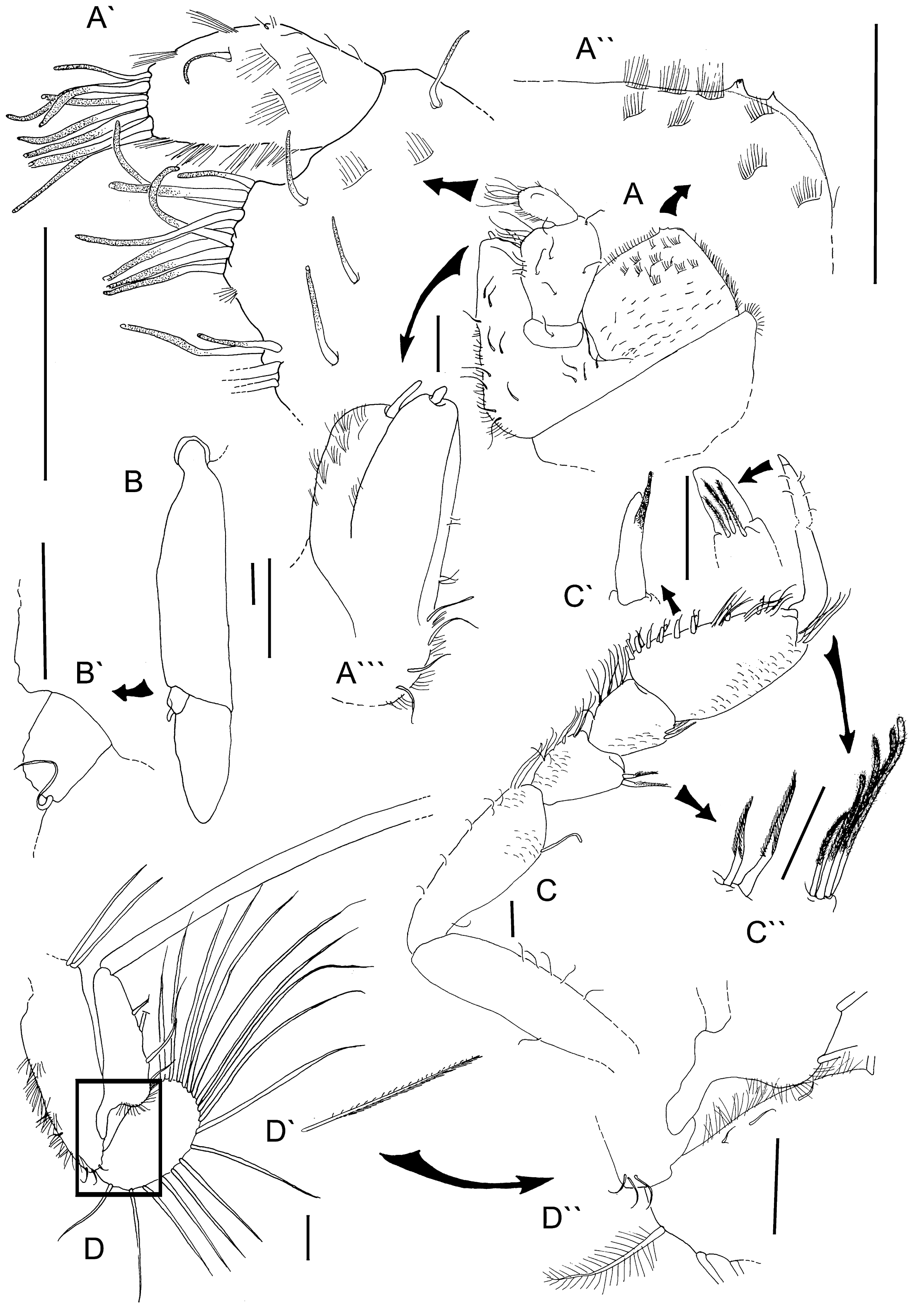

Figure 9. *Atlantoserolis vemae* Menzies, 1962, AMNH 12035, holotype male: maxilliped (A), with details of palpal tip (A′) and distolateral corner of epipodite (A″); uropod (B), with detail of exopod (B′); pereopod II (C), with detail of sensory setae and dactylar tip (C′) and distodorsal setae on merus and propodus (C″); pleopod 2 (D), with details of plumose seta (D′) and insertion of exopod and endopod on sympod (D″). Scale bars: 0.1 mm.

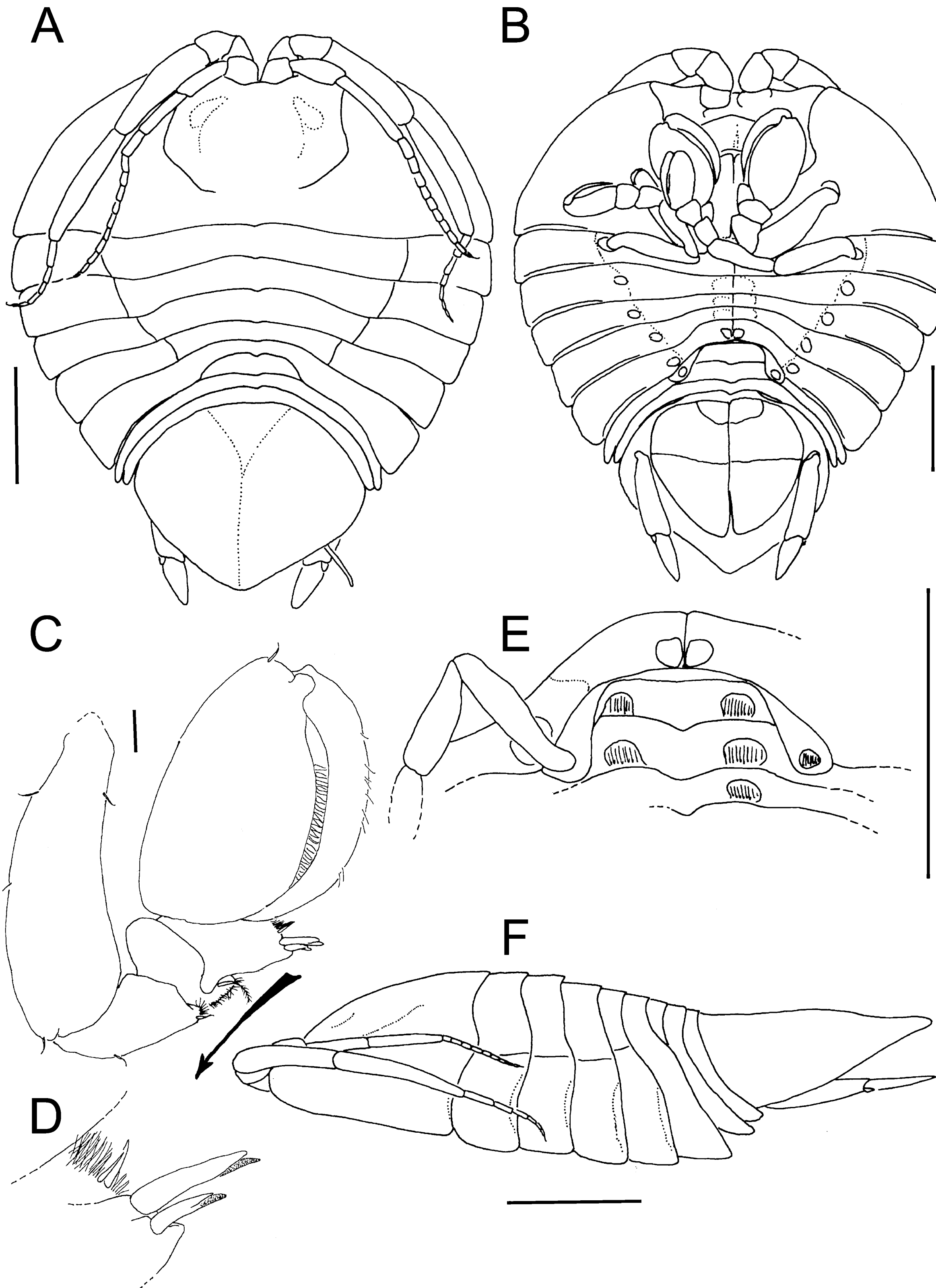

Figure 10. *Atlantoserolis vemae* Menzies, 1962, DIVA-3 material: dorsal (A) and lateral (B) views of male; pereopod I (C); setal composition of carpus tip of pereopod I (D); ventral view of pereonites (E); lateral view of pereonites (F). Scale bars: (a, b) 1 mm; (C–F) 0.1 mm.

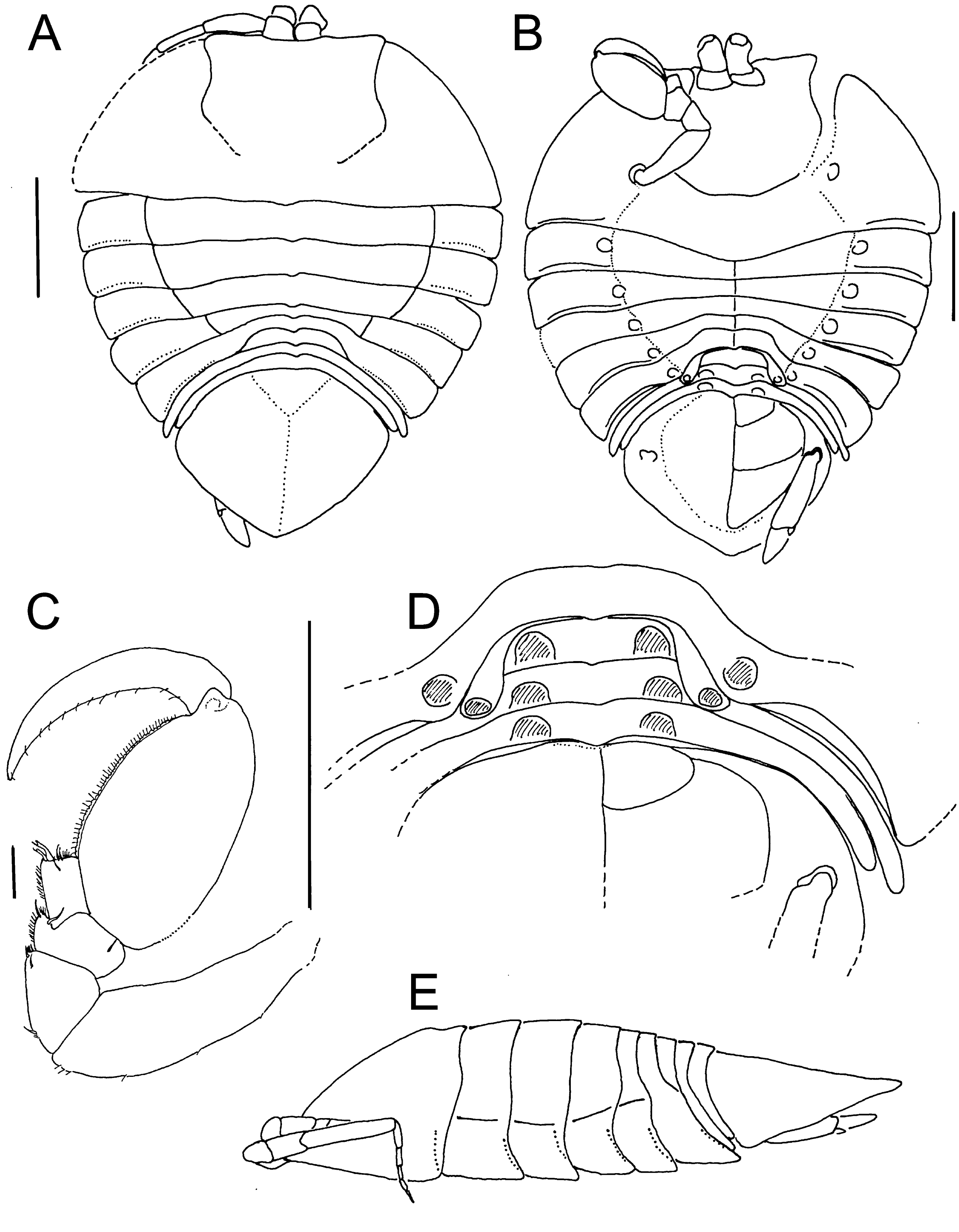

Figure 11. *Atlantoserolis vemae* Menzies, 1962, DIVA-3 material: dorsal (A) and lateral (B) views of female; pereopod I (C); detailed ventral view (D); detailed lateral view (E). Scale bars: (A–B) 1 mm; (C–E) 0.1 mm.

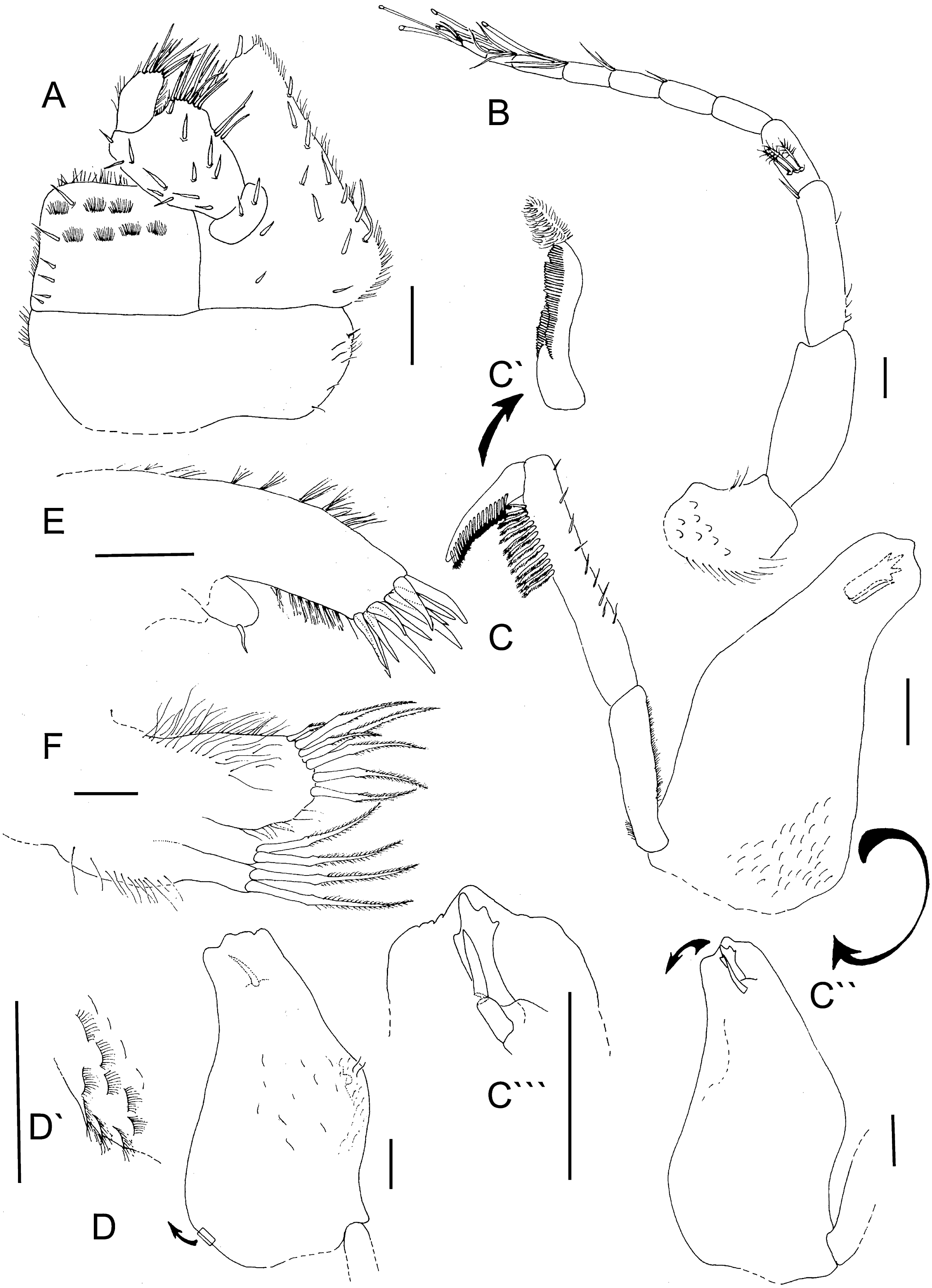

Figure 12. *Atlantoserolis vemae* Menzies, 1962, DIVA-3 material. Antenna mouthparts of female. Maxilliped (A), antenna (B), left mandible (C), enlarged seta of manibular palp (C′), left mandible, ventral view (C″), enlarged incisor and lacinia mobilis of left mandible (C‴), right mandible (D), setal combs of right mandible (D′). Scale bars: 0.1 mm.

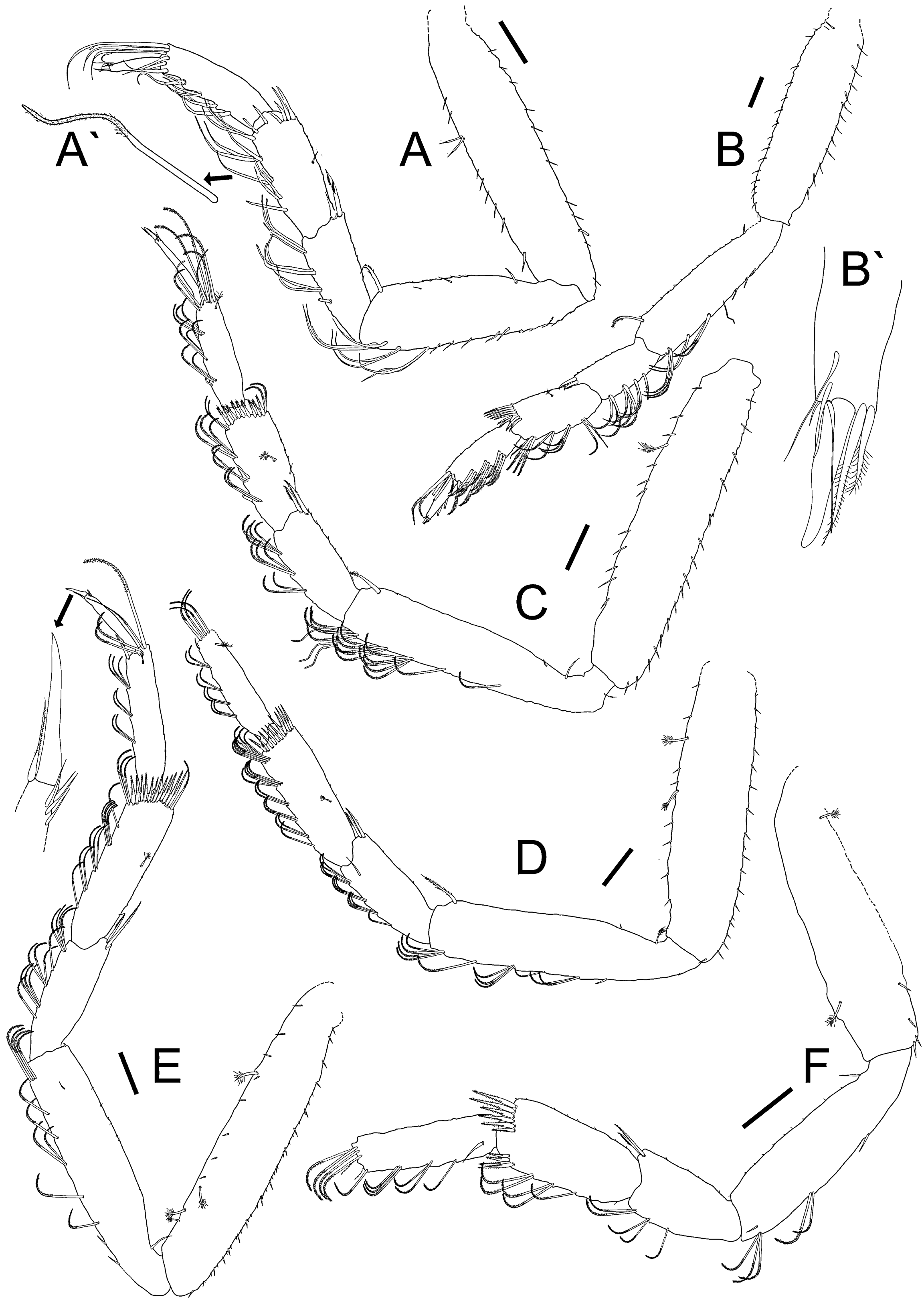

Figure 13. *Atlantoserolis vemae* Menzies, 1962, DIVA-3 material. Female pereopods II–VII (A–F), with details of ventral setae on carpus of pereopod II (A′) and tip of dactylus of pereopod III with dactylar claw (B′). Scale bars: 0.1 mm.

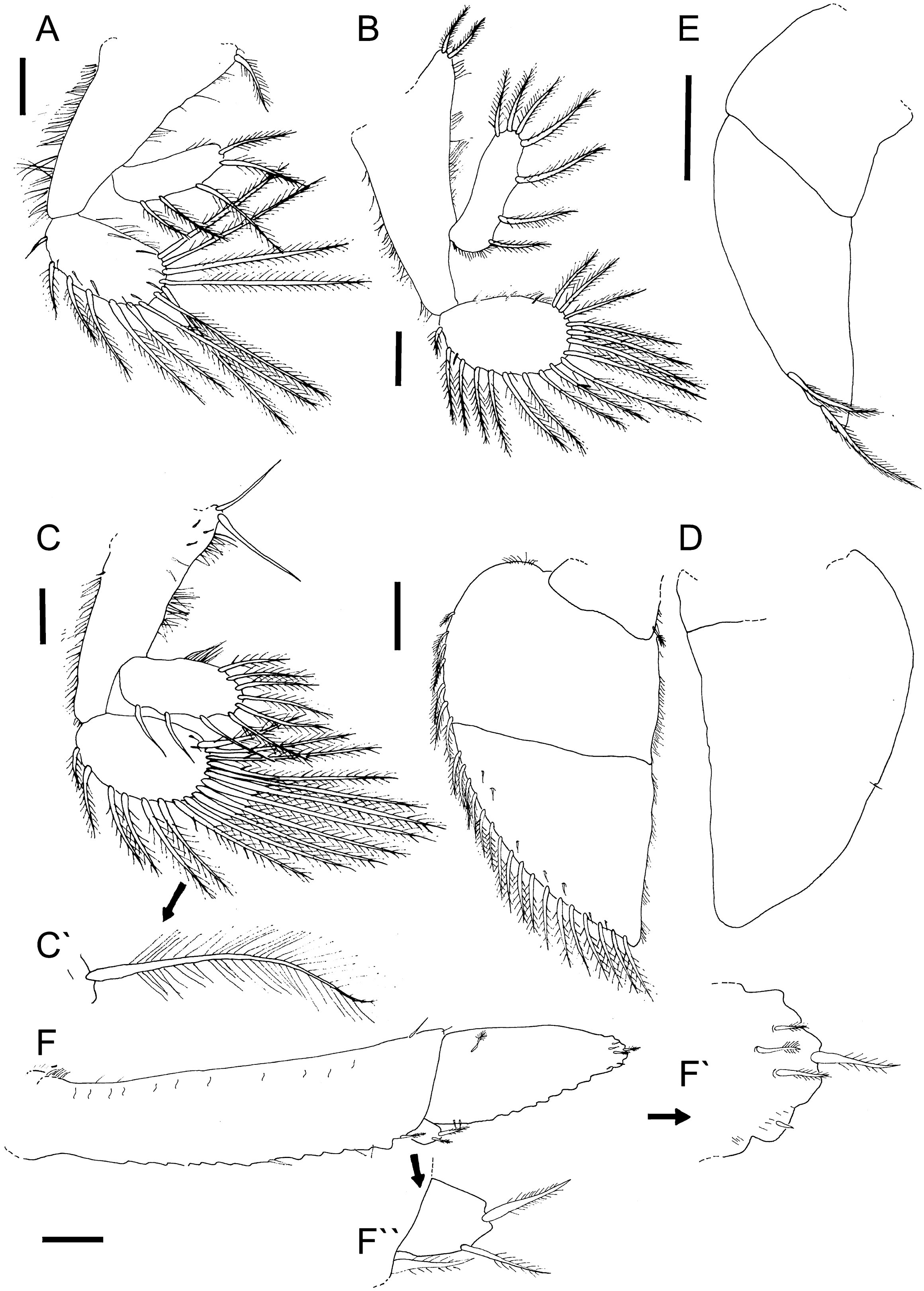

Figure 14. *Atlantoserolis vemae* Menzies, 1962, DIVA-3 material. Pleopods 1–5 (A–E), with detail of plumose seta (C′), and uropod (F), with details of endopodal (F′) and exopodal tip (F″). Scale bars: 0.1 mm.

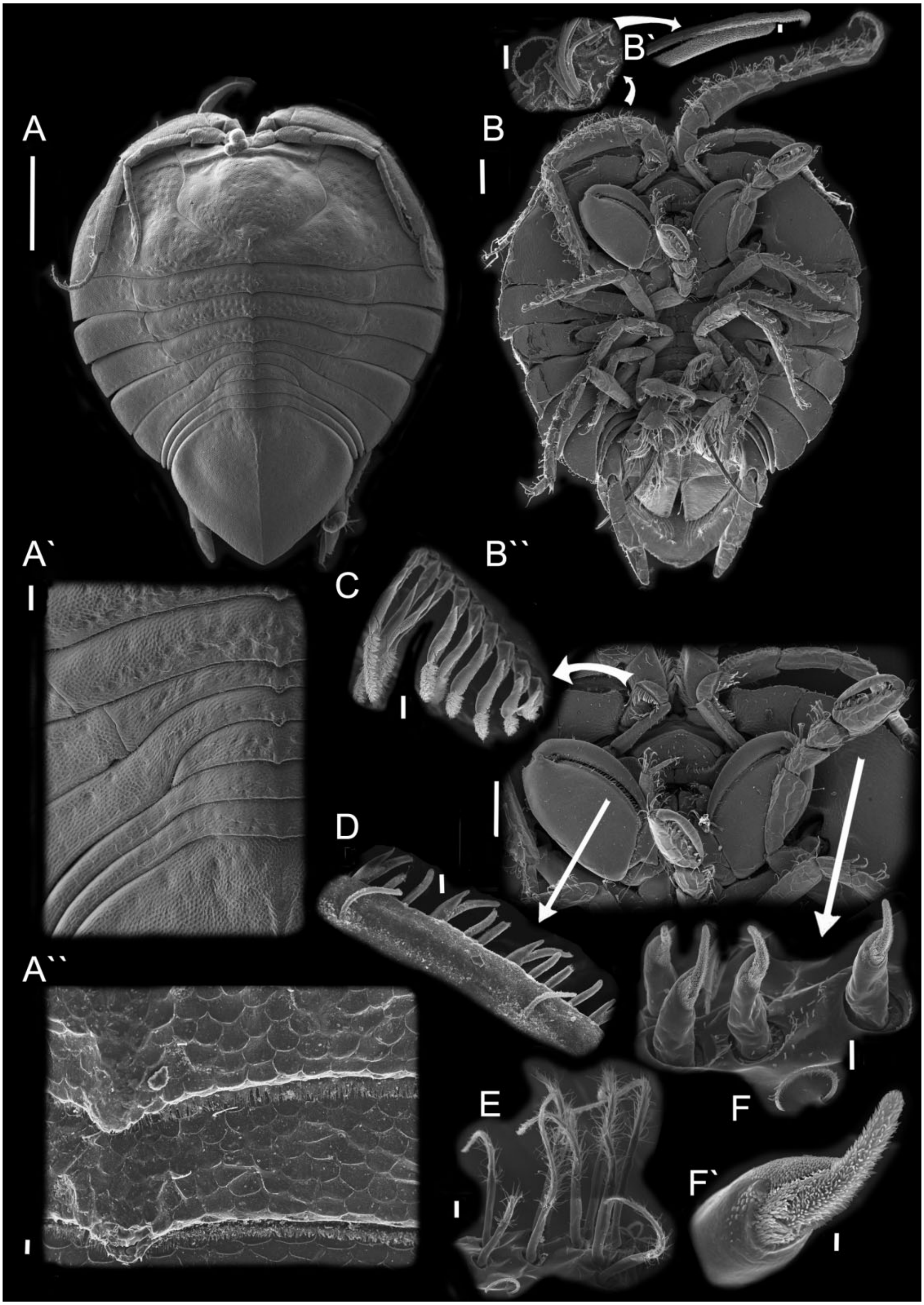

Figure 15. *Atlantoserolis vemae* Menzies, 1962 (DIVA-3) male SEM plate: A, habitus dorsal ZMH K-44076 (scale bar: 1 mm); B, habitus ventral ZMH K-44080 (scale bar: 300 µm); B′, detail of antenna, with bunch of setae at shaft densely covered with fringe-like setules; C, detail of pappose setae at mandible palp article 3; D, pereopod I propodus unequally bifid; E, detail of pereopod II carpus inner margin sensilla, pappose setae; F, F′ detail of pereopod I carpus inner margin unequally bifid setae with distally setules (scale bars: A′ 0.1 mm; A″, C–F, 0.01 mm; B′, 0.01 mm and 1 µm; F′, 2 µm). The habitus in dorsal view (A) shows epizoits (parasites) in the head area and on the uropod.

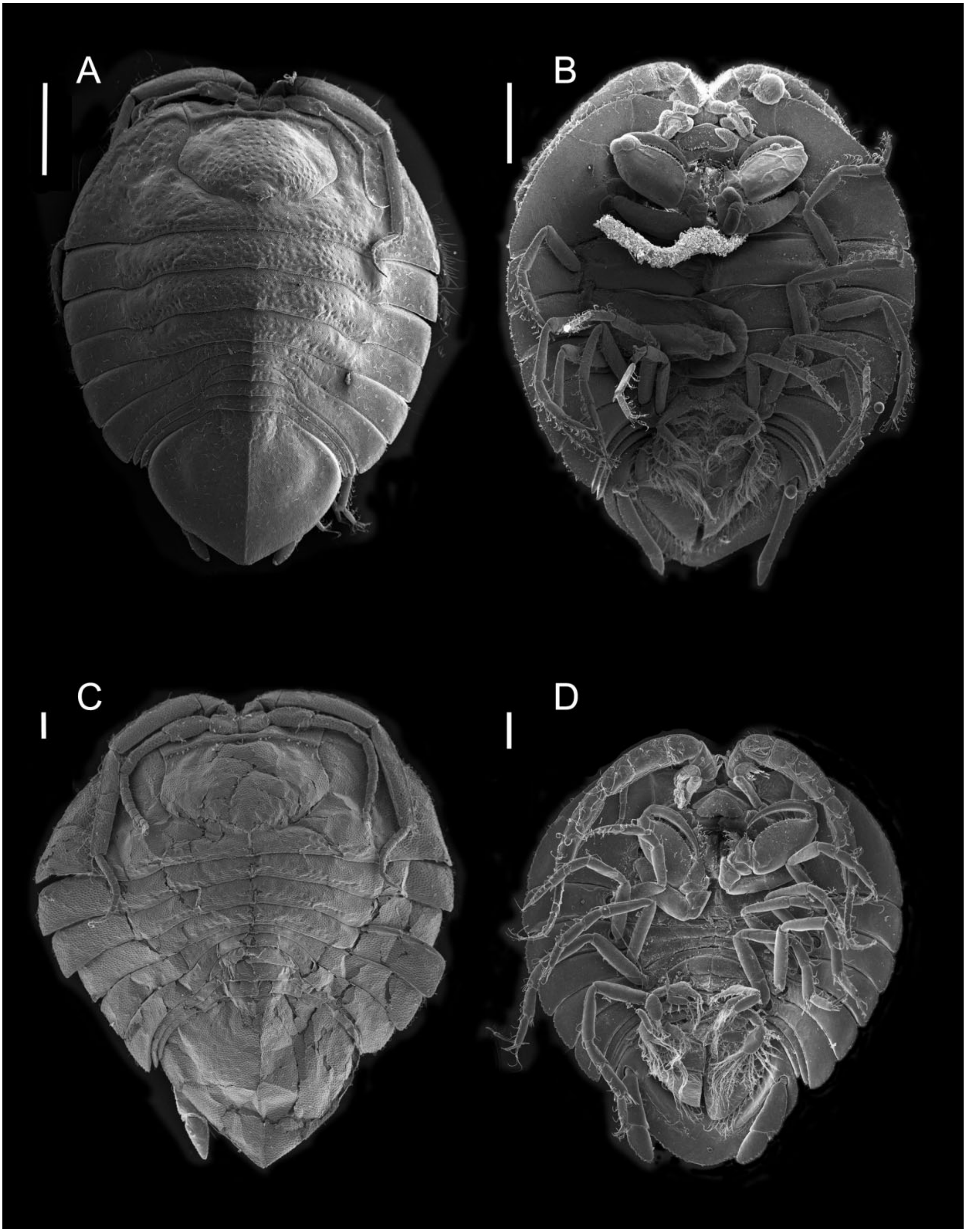

Figure 16. *Atlantoserolis vemae* Menzies, 1962 (DIVA-3) SEM plate. Female and juvenile habitus: A, female dorsal view ZMH K-44075; B, female ventral view ZMH K-44074; C, juvenile (stage according to Hessler, 1970) dorsal view ZMH K-44079; D, juvenile (stage according to Hessler, 1970?) ventral view ZMH K-44077. Scale bars: A, B, 1 mm; C, D, 200 μm. Ventral view of the female (B) with epizoits, especially on the mouthparts and antennae, as well as on pereonite 5 margin and the left uropod.

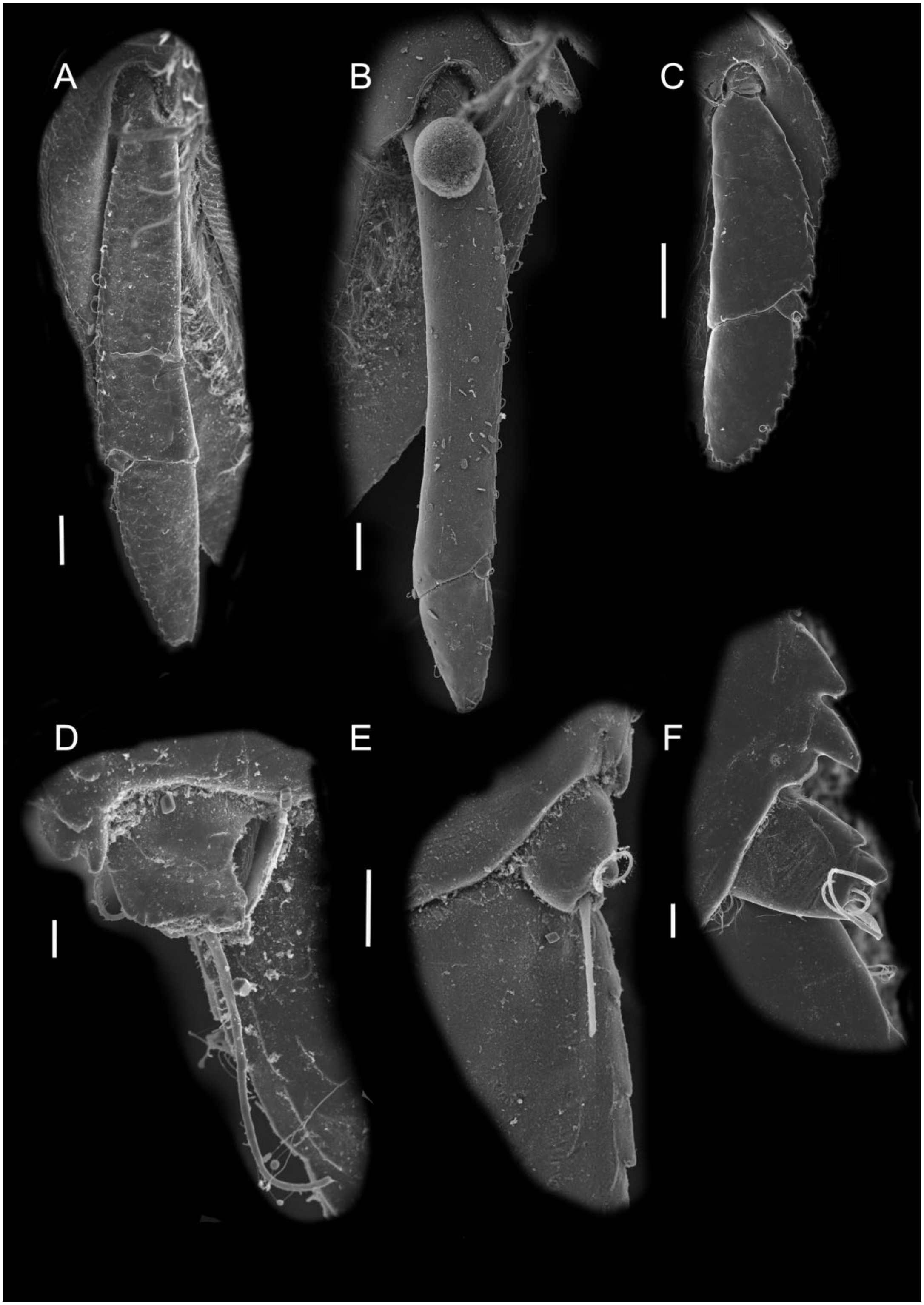

Figure 17. *Atlantoserolis vemae* Menzies, 1962 (DIVA-3) SEM plate. Uropods compared, from male, female, and juvenile. A, left uropod, male ZMH K-44080; B, right uropod, female DZMB HH 10275-1; C, right uropod, juvenile ZMH K-44077; D, detail of exopod, male ZMH K-44080; E, detail of exopod, female ZMH K-44074; F, detail of exopod, juvenile ZMH K-44077. Scale bars: A–C, 100 μm; D, F, 10 μm; E, 30 μm.

Figure 18. *Atlantoserolis vemae* (Menzies, 1962), confocal laser scanning microscopy images. ZMH K-44082, female : A, habitus dorsal; B, habitus ventral. Scale bars: 500 μm.

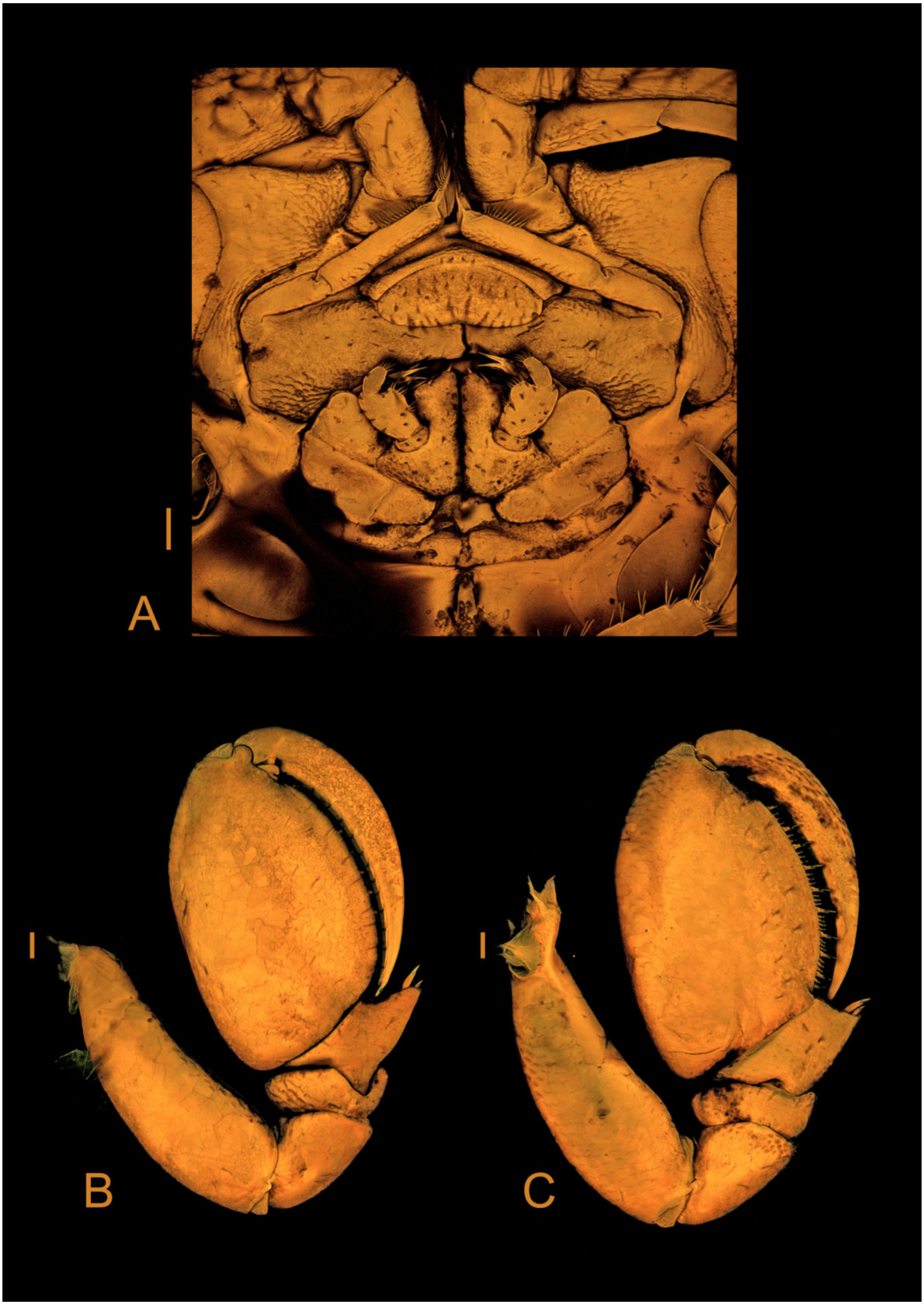

Figure 19. *Atlantoserolis vemae* (Menzies, 1962), confocal laser scanning microscopy images. ZMH K-44082, female: A, oral region; B, pereopod I (ventral view); C, pereopod I (dorsal view). Scale bars: A, 100 µm; B, C, 50 µm.

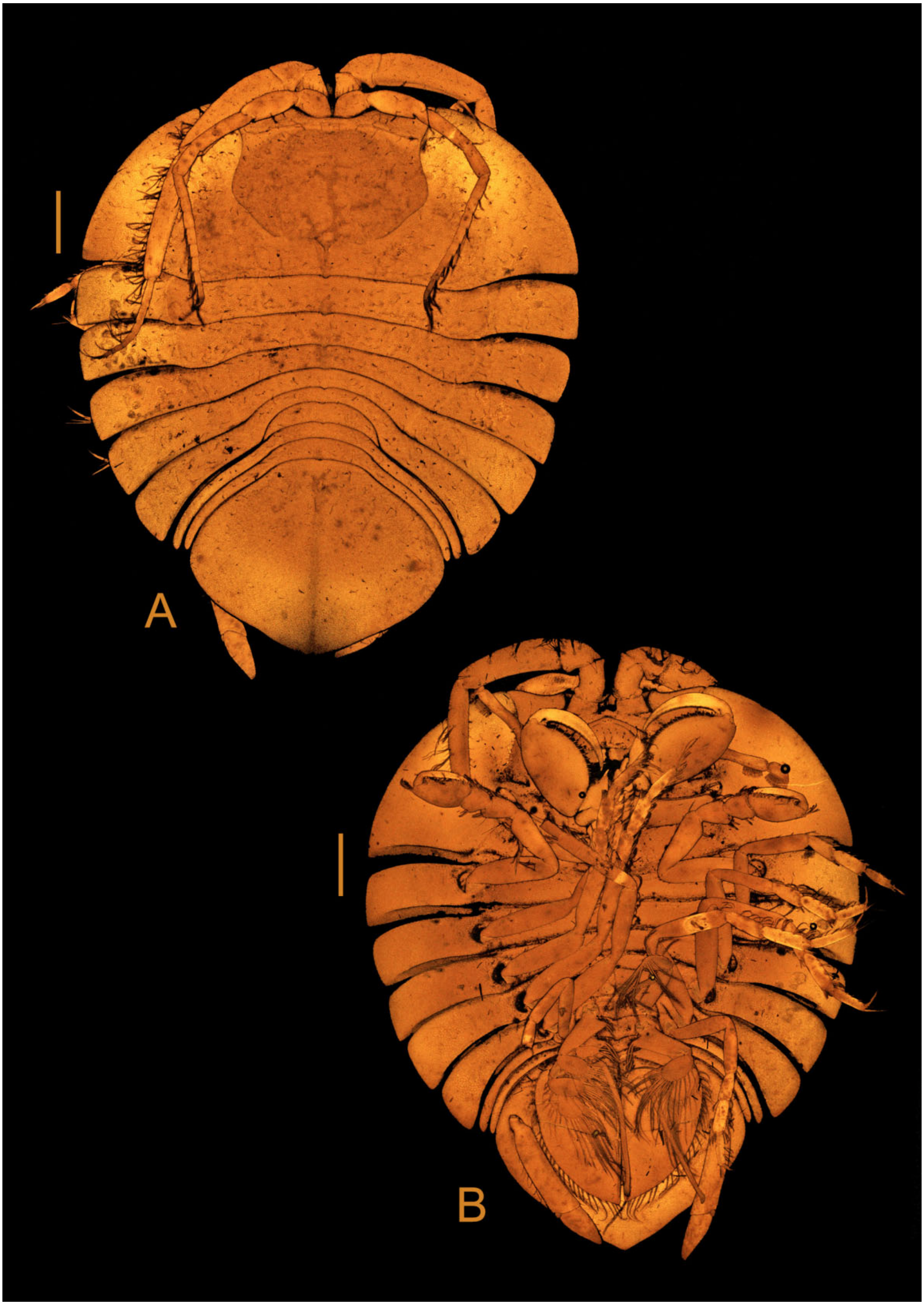

Figure 20. *Atlantoserolis vemae* (Menzies, 1962), confocal laser scanning microscopy images. ZMH K-44085, male: A, habitus dorsal; B, habitus ventral. Scale bars: 500 µm.

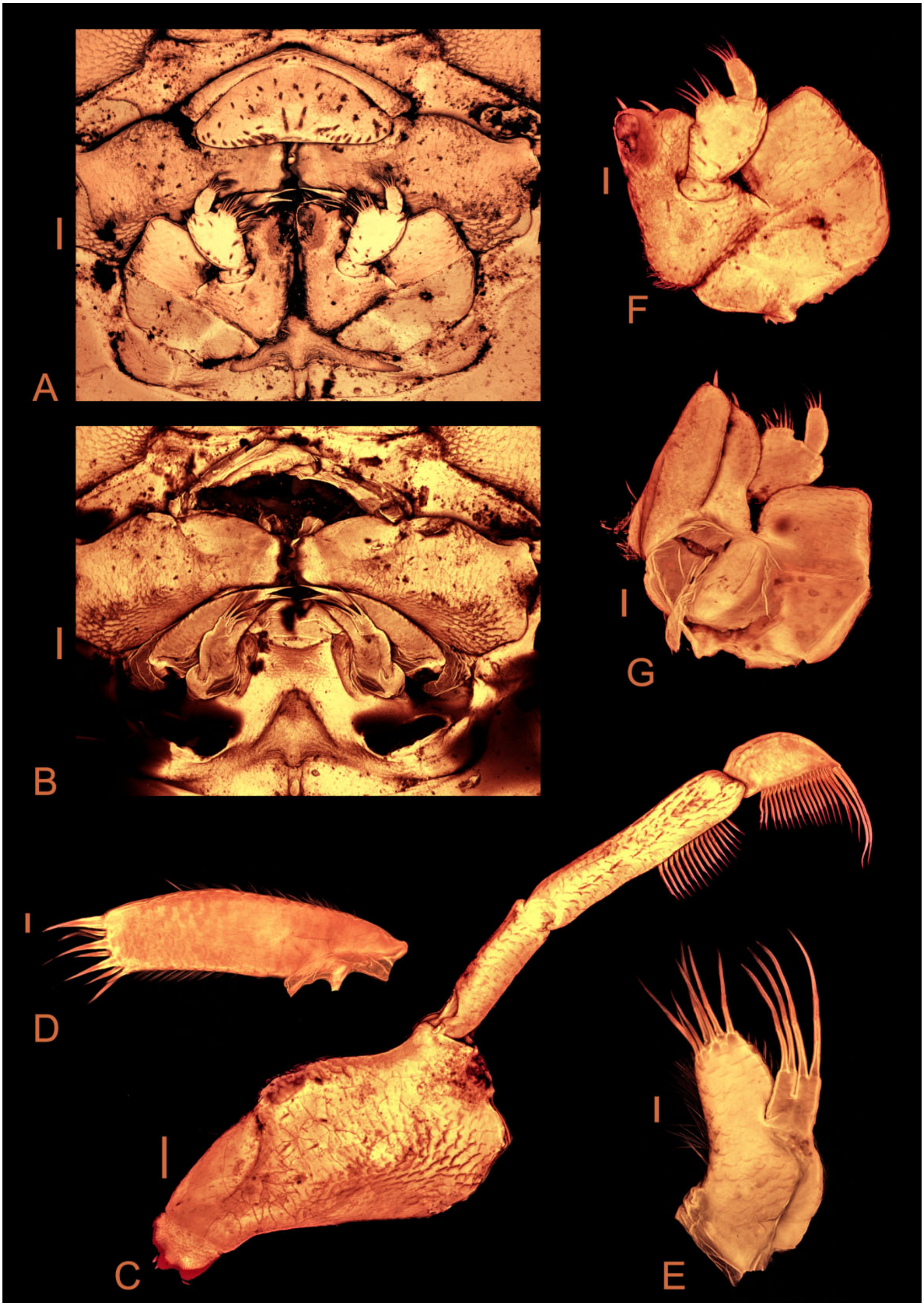

Figure 21. *Atlantoserolis vemae* (Menzies, 1962), confocal laser scanning microscopy images. ZMH K-44085, male. A, oral region; B, oral region, maxilliped, and labrum dissected; C, md; D, mxl; E, mx; F, mxp (ventral view) ; G, mxp (dorsal view). Scale bars: A, B, D, 100 µm; C, 75 µm; E, 25 µm; F, G, 50 µm.

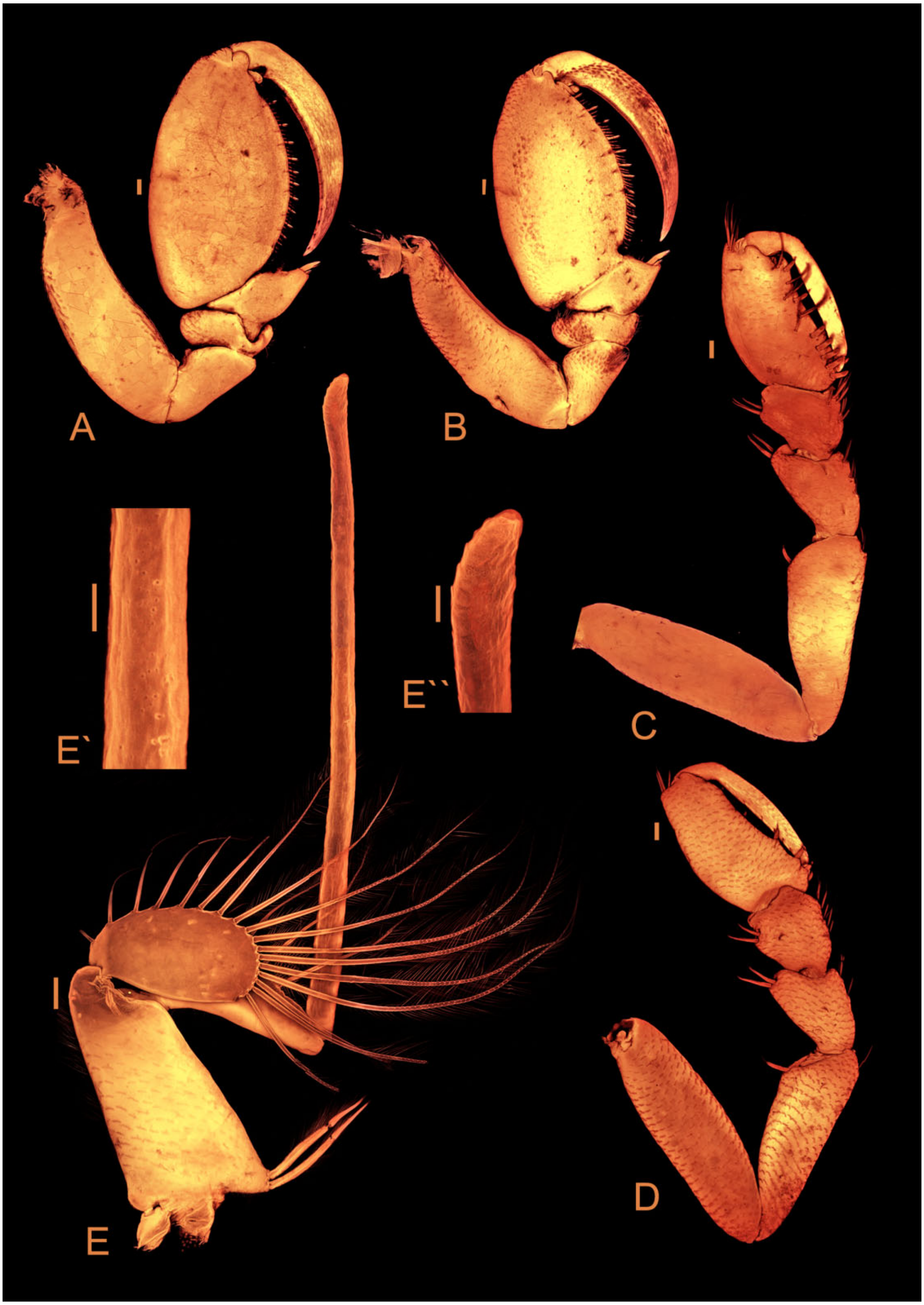

Figure 22. *Atlantoserolis vemae* (Menzies, 1962), confocal laser scanning microscopy images. ZMH K-44085, male: A, pereopod I (dorsal view); B, pereopod I (ventral view); C, pereopod II (ventral view); D, pereopod II (dorsal view); E, Plpo II, pleopod II; E′, middle part of appendix masculina with cuticular openings; E″, distal part of appendix masculina. Scale bars: A–E, 50 μm; E′, E″, 25 μm.

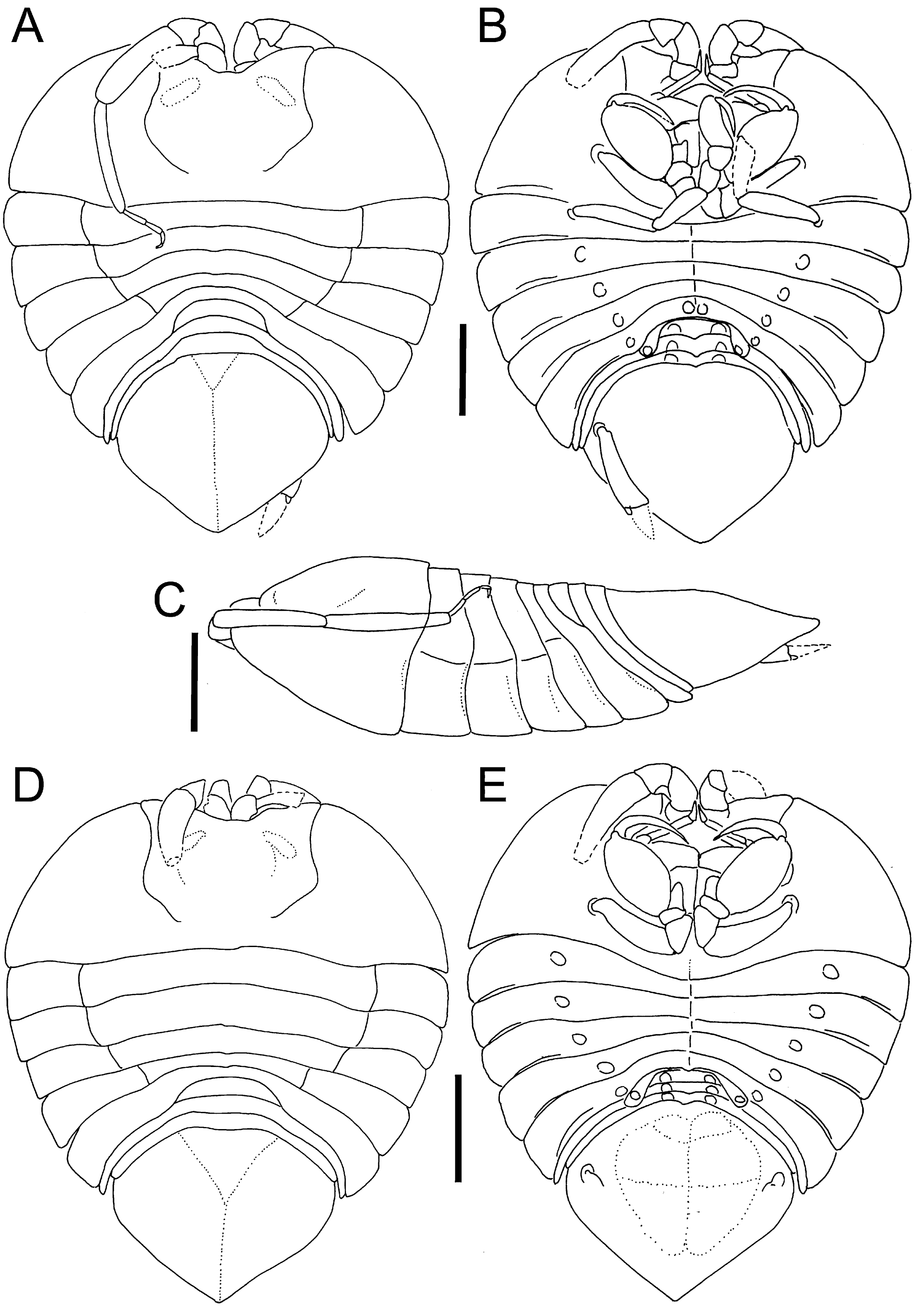

Figure 23. *Atlantoserolis vemae* (Menzies, 1962), specimens from the North Atlantic collected by R.R. Hessler 1967, 1970) at Woods Hole Oceanographic Institute station 70. Male from dorsal, ventral, and lateral views (A–C), and female from dorsal and ventral views (D, E).

Figure 24. *Atlantoserolis vemae* (Menzies, 1962), specimens from the North Atlantic collected by R.R. Hessler 1967, 1970) at Woods Hole Oceanographic Institute station 70. Confocal laser scanning microscopy images, female : A, habitus dorsal ; B, habitus ventral. Scale bars: 500 μm.

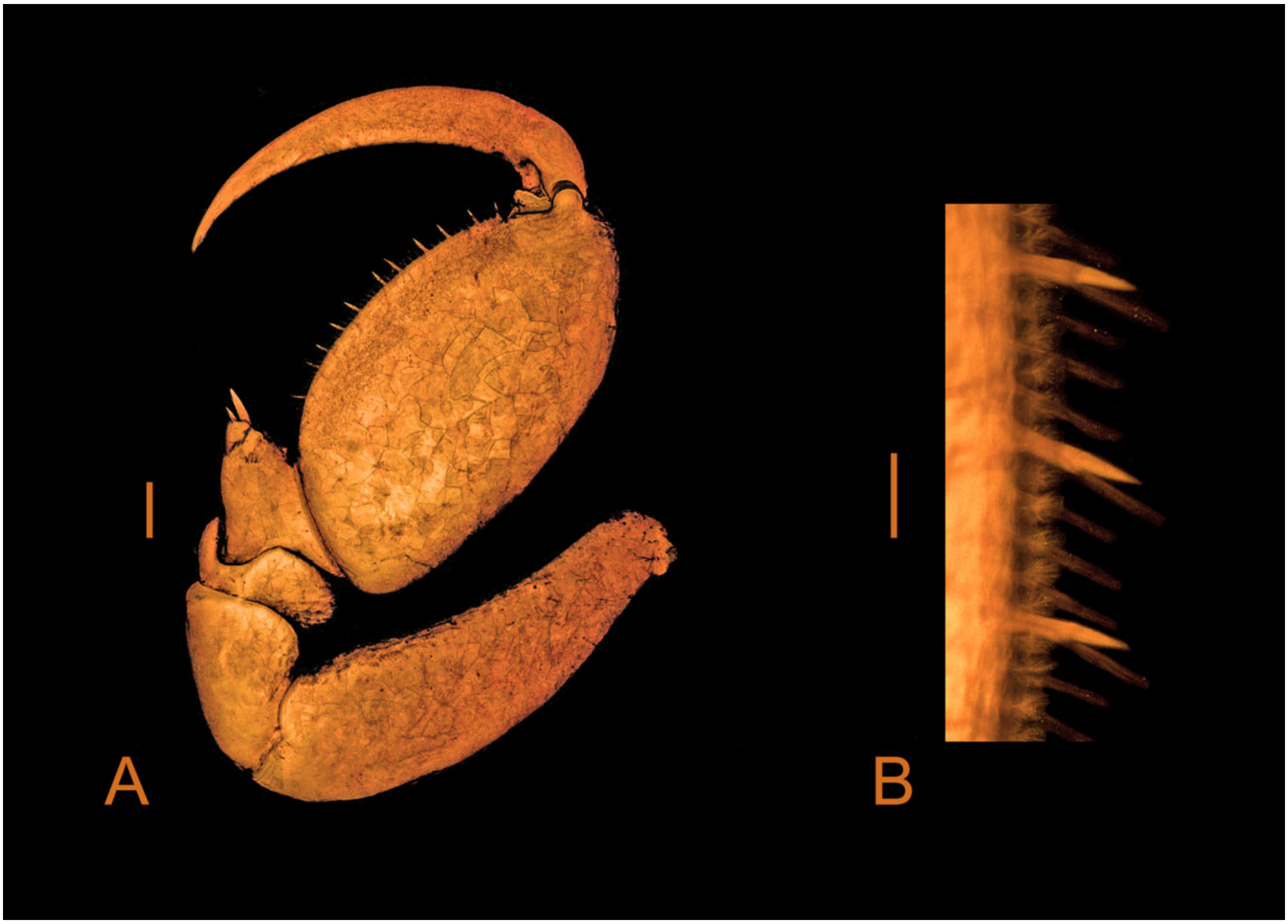

Figure 25. *Atlantoserolis vemae* (Menzies, 1962), specimens from the North Atlantic collected by R.R. Hessler 1967, 1970) at Woods Hole Oceanographic Institute station 70. Confocal laser scanning microscopy images, female: A, pereopod I (ventral view); B, detail of pereopod I. Scale bars: A, 100 µm; B, 25 µm.

articles without aesthetascs, last three articles with one aesthetasc each; articles 3–8 also with few simple setae of varying lengths. A2 (Figs 10, 15, 16, 18, 20) with short first, almost ring-like, peduncular article, second slightly more than twice as long as first, with few lateral short setules, third article slightly shorter than second, almost of triangular shape, with tufts of setae distally, fourth and fifth articles longest, fourth one broadest, both with tufts of setae, fifth 1.2 times as long as fourth; flagellum of nine articles, each with one or a group of distolateral simple setae, second flagellar article with one aesthetasc.

Mandibles (Figs 11, 19, 21) asymmetrical, right lacinia mobilis narrower than on left. Left lacinia mobilis a broad blade (with nine slight cusps indicated at serrated tip), almost as wide as incisor, spine (spine row rudiment) simple and straight. Right lacinia mobilis with four small teeth, spine simple and straight. Mandibular palp second article 1.6 times as long as first, with 16 short setae along distal part of lateral margin in left mandible (15 in right), third article lanceolate, with row of up to 19 setae (Fig. 21), last but one longest.

Maxilla 1 (Figs 12, 21) lateral lobe with 11 strong apical teeth; medial lobe stalked, small, distally rounded, with one short apical seta.

Maxilla 2 (Figs 12, 21) inner lobe with seven or eight simple slender setae and medial setules, median and outer lobes each with two setae.

Maxilliped (Figs 9, 12, 19, 21): coxa and epipod lateral to it separated by suture; basis separated by suture from lateral rounded lamella; basis with facial setae and small setules near mesial face; endite with transverse distal margin bearing two spiniform setae mediodistally, placed on two lobes, medially simple setae and fine, small setules; palp with short, ring-like, first article, second article with five stronger lateromedial setae, long medial setae and four ventral setae, third article with distal tuft of setae.

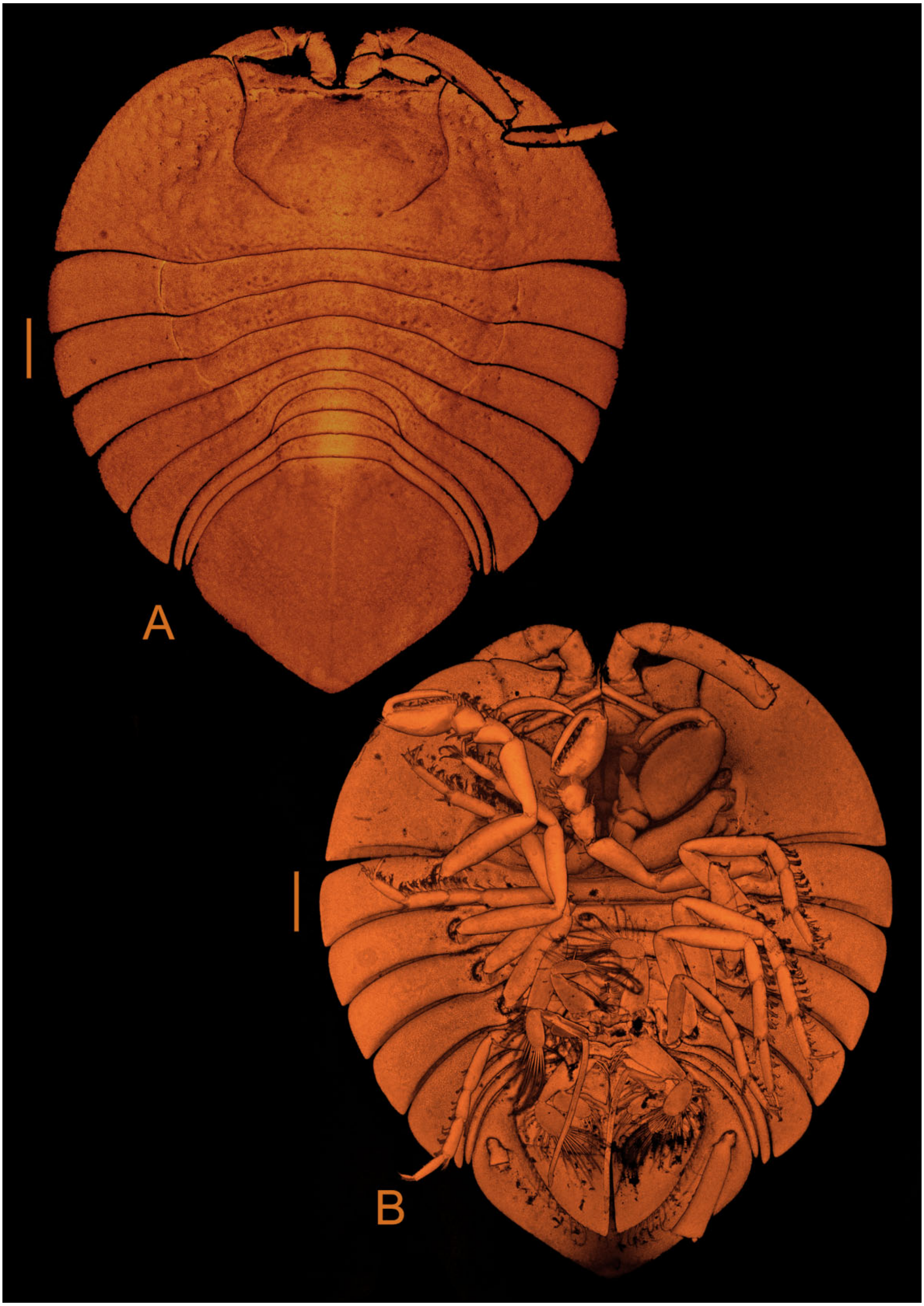

Figure 26. *Atlantoserolis vemae* (Menzies, 1962), specimens from the North Atlantic collected by R.R. Hessler 1967, 1970) at Woods Hole Oceanographic Institute station 70. Confocal laser scanning microscopy images, male: A, habitus dorsal ; B, habitus ventral. Scale bars: 500 µm.

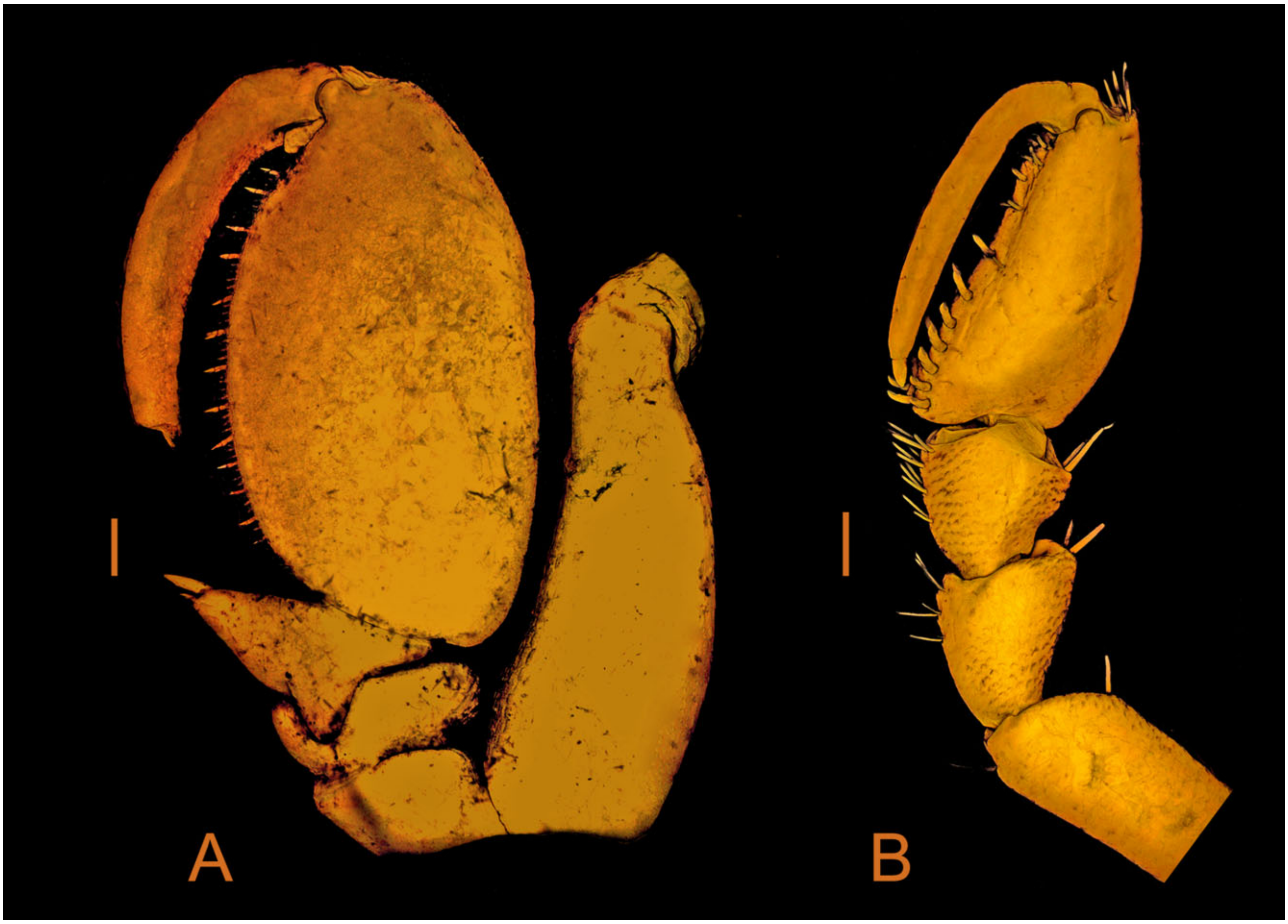

Figure 27. *Atlantoserolis vemae* (Menzies, 1962), specimens from the North Atlantic collected by R.R. Hessler 1967, 1970) at Woods Hole Oceanographic Institute station 70. Confocal laser scanning microscopy images, male: A, pereopod I (ventral view); B, pereopod II (ventral view). Scale bars: 100 μm.

Pereopod I (PI; Figs 7, 10, 11, 15, 16, 18, 19, 20, 22–27) basis to merus with simple short setae and setules; carpus quadrangular, with two simple and two strong sensory setae mediodistally; propodus long–oval, widest at midlength, curved palm with row of alternating fan-shaped setae and shorter setulated sensory setae, each with apical projection, and submarginal lateral row of short simple setae; dactylus evenly curved and tapering, without claw.

Pereopod II (PII; Figs 9, 10, 15, 16, 18, 20, 22, 23, 24, 26, 27) with basis 1.4 times longer than ischium, few simple short setae and two distomedial plumose setae; ischium with row of ventral simple setae, in distoventral third these are very long; merus about half as long as ischium, with more long ventral setae, carpus as long as ischium, also with ventral simple setae, ischium and carpus with distodorsal strong setae, carpus also with lateral setae; propodus about as long as carpus (0.94), also with ventral and distolateral and distodorsal row of two long setae, distal setae longer than dactylus; dactylus half the length of propodus, almost straight, just surpassing heel of palm, unguis not differentiated, four distal setae, one longer distoventral seta.

Pereopods III–VII (Figs 13, 15, 16, 18, 20, 24, 26) similar, distal articles of posterior limbs longer. Basis, ischium, and merus of similar shape; carpus as long or slightly longer than merus, setose on ventral margin; propodus shorter than carpus, carpus slightly longer than merus, all articles from distal third of ischium to propodus setose on ventral margin, with long setae on palm; dactylus very slender, 0.5 times width and 0.6 times length of propodus, tapering.

Pleopods 1–3 (Figs 9–11, 14–16, 18, 20, 24, 26) peduncle broad, almost triangular, with medial lobe bearing oneor two setulate setae; endopod round–oval, with 13–17 marginal plumose setae; exopod long–oval, also surrounded with between five and nine marginal plumose setae. Plp 4 (Fig. 14) exopod operculiform, chitinized, bi-articulate, with lateral row of more than 100 short marginal plumose setae; endopod smaller, distally with four setae. Plp 5 (Fig. 14) smallest (damaged during dissection), exopod weakly biarticulate, with two distal plumose setae; endopod (broken off during dissection) almost as long as exopod, without setae.

Uropod (Figs 8–11, 14–18, 20, 23) attached after two-thirds of Plt length, slightly surpassing distal tip, with elongated quadrangular peduncle, bearing few simple setae; rami oval, exopod small, 0.15 times length of endopod, distally rounded, with two setulated setae; endopod twice as long as wide, distally rounded, distally and laterally serrated, with a few small distally setulated setae and small and short simple setae.

Male (only sexually dimorphic characters): Cuticular structures (ornamentation by small scales) more coarse in males than in females, male generally slightly more setose, with more simple short setae on many appendages, although shape and proportions do not differ much unless expressed in the following. Peduncular articles of A1 broader and more robust than in female. Left mandible and PI (Figs 8, 15, 21) similar to female, but PII differs from female (Figs 9, 22, 27), subchelate, with long and slender basis, bearing five dorsal and one ventral simple setae; ischium 0.8 times as long as basis, merus and carpus of equal length, one-third the length of ischium, all three articles with ventral simple setae, long simple setae also distoventrally on ischium, carpus, and propodus; propodus slightly triangular, proximally widest, distally slightly narrowing, with proximoventral strong sensory setae, medio- and distoventrally more slender simple setae, simple setae in ventral distal half long; dactylus fitting between ventral row of setae, reaching tip of propodus protrusion in ventral view, palm of propodus with five long simple setae. Plp 2 (Figs 9, 22) peduncle with more lateral simple setae than in Plp 1, with narrow medial lobe bearing two rather long setulate setae (possibly because of medially protruding appendix masculina); endopod broader than in Plp 1, with four marginal plumose setae, with long apical slender appendix masculina, more than 14 times as long as endopod; exopod larger, broader, also with marginal plumose setae. Uropod (Figs 9, 17) very similar to female, but endopod without serrated margin and without setae.

Distribution

North and South Atlantic (Fig. 1), depth 4588–5024 m.

Remarks

Atlantosolis vemae (Menzies, 1962) can easily be distinguished from *A. venusta* (Moreira, 1977) by the lack of spines. Its body surface shows some ornamentation, with small scales, whereas in *A. venusta* a pronounced median carina extends mediocaudally into a pointed tip (the Plt is triangular in shape). Moreover, *A. vemae* has a broader and laterally more rounded (although caudally slightly acuminating) Plt, which is almost straight and triangular in shape in *A. venusta*. The body surface of *A. agassizi* (George, 1986) is also smooth, but the Plt is round–oval in shape and broadly rounded caudally. In *A. venusta* the uropods are extending the length of the Plt and are superficially uniramous (Moreira, 1977), sympod and endopod are fused, exopod is freely articulated; however, it is obscure and minute, and inserts at one-third the uropodal length from tip. The uropods of *A. vemae* possess an endopod of one-third the length of sympod, the exopod is small, a sixth of the size of the endopod, almost quadrangular, and bears one distal seta. *Atlantosolis agassizi* has similar shaped uropods; however, the articles are more robust, the lateral margins of sympodites are serrated and saw-like, and not smooth as in *A. vemae*, the endopodite bears two distal setae, and the exopod is smaller (0.15 times the endopod), and does not bear any setae. According to Hessler (1970), *A. menziesi* (Hessler, 1970) can best be distinguished from *A. vemae* in the shape of the uropods, which are similar in shape to those of *A. venusta*. In the juvenile specimens, the uropod is more robust, shorter, and possesses an almost saw-like lateral margin. The uropod of *A. menziesi* is straight compared with that of *A. venusta*, which is medially and laterally faintly curved. The Plt of *A. venusta* only bears a medial keel, whereas in *A. menziesi* it is characterized by a frontomedial distinct triangular elevation, continuing into a keel extending to caudal tip.

Molecular results

The only *Glabroserolis* specimen (KJ119, DZMB-HH 14823) is genetically distinct compared with the *Atlantoserolis* material in our study (*18S*, > 3.8% uncorrected pairwise distance; *16S* and *COI*, > 20% uncorrected pairwise distance). The distribution of pairwise genetic distances (K2P) within *A. vemae* followed a pronounced bimodal distribution in all three genes (*16S*, ≤ 0.025 and ≥ 0.047; *COI*, ≤ 0.04 and ≥ 0.089; *18S*, ≤ 0.0007 and ≥ 0.0046). Using 18 families of Crustacea, Lefebure *et al*. (2006) reported an intraspecific mean for the *COI* gene of 0.013 versus 0.154 among closely related but reproductively isolated species, and 0.021 versus 0.037 for the *16S* gene (see also Held, 2000). The magnitude and pattern of the genetic differentiation among *A. vemae* are thus in line with expectations from genetically isolated species in Crustacea (Held, 2003; Held & Wägele, 2005; Lefebure *et al*., 2006).

Although the magnitude of differentiation between the two groups differs among the genes according to their evolutionary speed, there is no conflict among them,

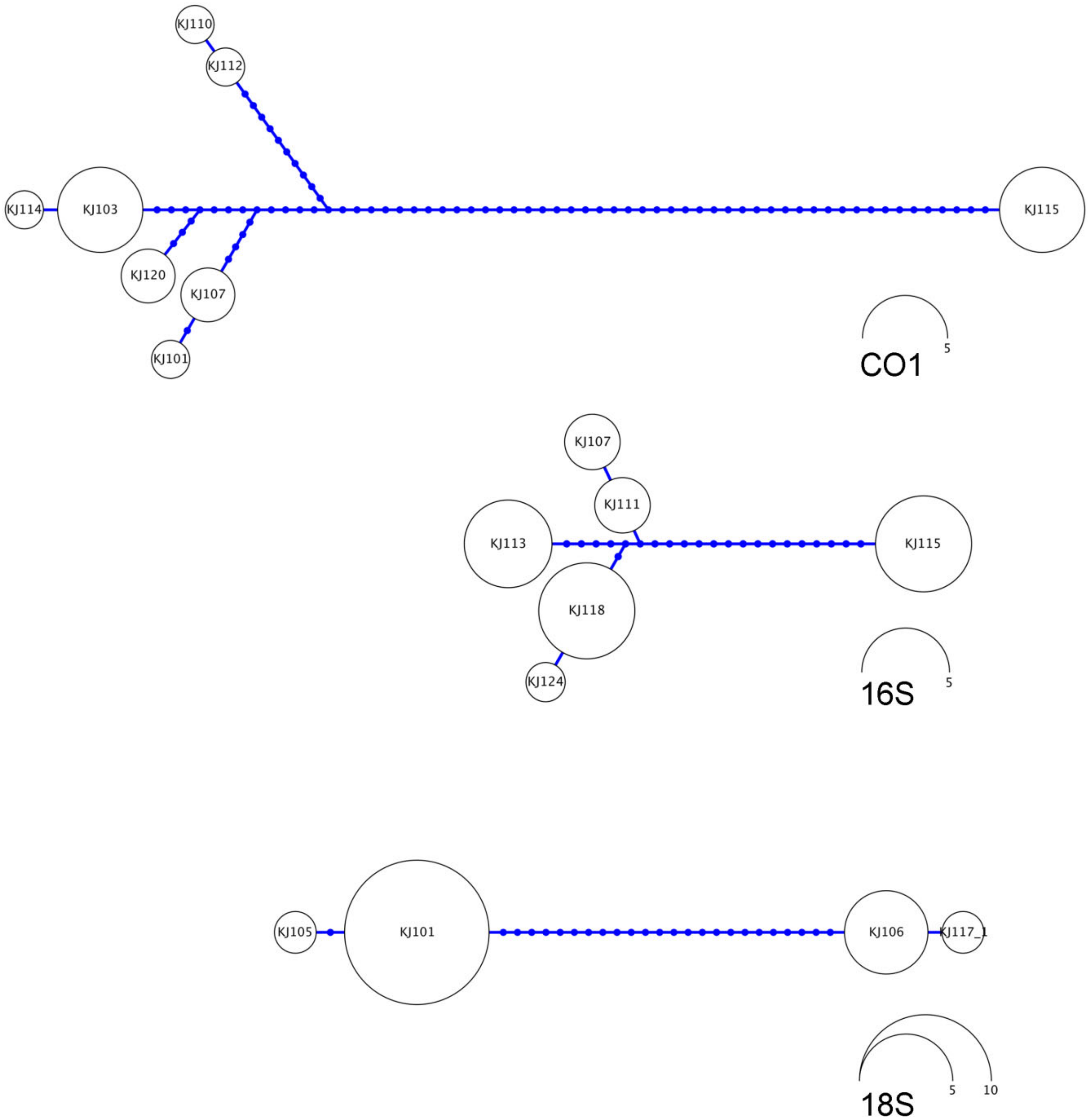

Figure 28. Molecular results for *COI*, *16S*, and *18S*: haplotype networks. Circles show the expedition identification number (compare with Table 3).

i.e. the specimens are sorted into genotype groups that are congruent among all three genes. Three juveniles (DZMB IDs-14819/KJ115, 14820/KJ116, 14821/KJ117), one male (DZMB ID-14810/KJ106) of 4 mm in length, and one female (DZMB ID-14826/KJ122) of 4.5 mm in length, obtained at DIVA-3 station 534, clustered together to the exclusion of all other *A. vemae* specimens from the same epibenthic sledge (EBS) deployment (Fig. 28). Because of failures of amplification or because of exclusion during the quality control steps, as described in the Material and methods section, we do not have sequence data for all genes for all specimens; however, the remaining specimens could be placed unequivocally in either of the two genotype groups based on the partial sequence information available (data not shown).

We observed no frame-shift mutations or occurrence of stop codons in the protein-coding *COI* gene and no extraneous sequence reads in any of the other genes. Although this observation does not completely rule out pseudogenes or nuclear copies of mitochondrial DNA (numts) as a possible explanation (Buhay, 2009), we are confident that the unexpected genetic diversity is not an artifact, but a real characteristic of the population under study that needs explaining.

DISCUSSION

The morphological differentiation among the *Glabroserolis* and *Atlantoserolis* in our study is mirrored in the differentiation of their mitochondrial and nuclear DNA markers. More surprising, however, is the fact that all three markers (*16S*, *COI*, and *18S*) identify two genetically highly differentiated groups among the *Atlantoserolis* specimens from DIVA-3 (Fig. 28). Recent studies have shown that the presence or absence of the so-called barcoding gap is sensitive to sampling error, both with respect to the total sample size as well as the geographical coverage of the sampling, compared with the total distribution of the species (Bergsten *et al*., 2012). Although the total sample size of *Atlantoserolis* included in our study may be on the high side of what is typically available for epibenthic macrofauna from the deep-sea (Brandt *et al*., 2007), the fact that most of our samples originate from a narrowly defined geographic area precludes a conclusive statement about the absence of intermediary values of genetic differentiation (i.e. presence of a barcoding gap); however, *A. vemae* from the North Atlantic (redescribed by Hessler, 1970; Figs 23–27) differs in having a slightly shorter second, compared with first, pleopodal epimer in females, but this is not a character allowing the description of a new species. Unfortunately, because of formalin fixation, no DNA could be extracted from the Hessler material of the USNM. Molecular genetic studies of freshly collected material of *A. vemae* from this site from the North Atlantic are needed in order to clarify whether the material that Hessler (1970) redescribed is in fact *A. vemae*, or whether it is a new species.

The magnitude of genetic differentiation, the strictly bimodal distribution of pairwise genetic differentiation values, the agreement among three different genes (nuclear as well as mitochondrial), and the persistence of two distinct gene pools in sympatry are easier to explain assuming the presence of two reproductively isolated species within the DIVA-3 *A. vemae* specimens, which cannot (yet) be discriminated morphologically, than assuming a single, genetically strongly differentiated species.

The dispersal abilities of deep-sea isopod species might be strongly influenced by geographic barriers and oceanographic conditions (Brix & Svavarsson, 2010), depending on their swimming abilities (Schnurr *et al*., 2013). It has recently been shown that at least some strictly benthic isopods were capable of long-distance dispersal (Leese *et al*., 2010; Brix *et al*., 2011; Riehl & Kaiser, 2012), although they were brooders with limited dispersal abilities. *Atlantoserolis vemae* was first recorded by Menzies (1962) from the South Atlantic, then by Hessler (1969, 1970) from the North Atlantic. Hessler (1969) included drawings of all developmental stages of a complete growth series and counted the number of each state found at WHOI station no. 70. At present, nominal *A. vemae* occurs with a pan-Atlantic distribution, but is often absent from samples between the North and the South Atlantic populations (Fig. 1). The geography of the South Atlantic has been reviewed by Wefer *et al*. (1996). The South Atlantic is fed by water from the North Atlantic at mid-depth ranges, and receives its densest water from the Weddell Sea (Reid, 1996). The Argentine Basin is 6212 m deep and influenced by Antarctic bottom water from the Southern Ocean Weddell Sea, eastwards it is framed by the Mid-Atlantic Ridge (MAR), and westwards by the South American shelf (Reid, 1996). The Rio Grande Rise separates it from the Brazilian Basin in the north, which reaches a maximum depth of 6537 m, and is characterized by soft substrate and a small number of trenches connecting to neighbouring deep-sea basins (Hogg *et al*., 1996). The circulation in the deep Brazilian Basin has been described by Hogg *et al*., 1996). To the south, there is a boundary between the South Atlantic and the Southern Ocean formed by the Drake Passage, with current velocities of the Antarctic Circumpolar Current of up to 130 Sv (Webb, 1996). Most studies, however, focused on large-scale observations of geology and oceanography of the Atlantic Ocean, rather than the biology of species (Wefer *et al*., 1996; Thistle, 2003); however, if the interaction of water masses and currents allow *A. vemae* pan-Atlantic dispersal, this would have most likely occurred from the south, supported by the Antarctic bottom water spreading north into the South and North Atlantic (Brandt *et al*., 2007). We suggest – although we cannot yet prove – that the North Atlantic *A. vemae* specimens described by Hessler are most probably another species, because of the geographic distance and the reduced gene flow as well as known cryptic speciation within Serolidae (Held, 2003; Leese *et al*., 2008; but see Leese *et al*., 2010). Moreover, we already observed differences in the *COI* gene sequences in the South Atlantic material and the absence of intermediate samples connecting both populations, indicating potential continuing speciation processes. Unfortunately, it was very difficult to identify any morphological differences.

Such problems, however, are also reported for other deep-sea isopod families like Haploniscidae (Brökeland, 2010; Brix *et al.,* 2011) and Desmosomatidae (Brix *et al*., 2014; Brix, Savarsson & Leese, 2014), which show high intraspecific genetic variability (7.5% in *16S* and 12.2% in *COI*) within one morphospecies. In contrast, another desmosomatid species shows high genetic similarity among specimens from the Brazilian Basin and the Guinea Basin, suggesting continuing gene flow across the Mid-Atlantic Ridge (Brix *et al*., 2014).

The unusual inheritance of mitochondria can, under certain circumstances, mimic strong genetic differentiation, and can incorrectly lead to the belief in the presence of two or more species when there is really only one. Some bivalve molluscs are known to harbour co-existing and strongly differentiated mitochondrial genomes in their cells, which are inherited separately in both sexes, a phenomenon called doubly uniparental inheritance (Passamonti & Ghiselli, 2009). Both of the operational taxonomic units (OTUs) of *A. vemae* that we describe here contain males and females, and are furthermore characterized in an identical composition by the nuclear *18S* gene; hence, we can exclude doubly uniparental inheritance as an explanation of our observation.

The co-existence of two genetic clusters (mitochondrial as well as nuclear) in which the levels of differentiation exceed the expectations for intraspecific differentiation is even more surprising considering that in our genetic approach we studied material originating exclusively from a single station (one EBS deployment); however, we were unable to identify diagnostic characters in the morphology of the two OTUs, despite the fact that all specimens were only minimally damaged during DNA extraction and were carefully examined in their morphology. We conclude that the two OTUs therefore either represent a single species, which for unknown reasons is clearly differentiated, or that the two OTUs may be two species, which are genuinely cryptic rather than pseudo-cryptic (Janosik & Halanych, 2010). Although there may be good reasons to flag potentially new species to attract further attention (Wägele, 1994), we do not propose the formal erection of a new species here because it can currently only be reliably identified a posteriori by DNA sequencing.

ACKNOWLEDGEMENTS

We are grateful to the crew of RV *Meteor* and to all pickers and sorters at sea. The sorting of the DIVA-3 material took place in the laboratories of the DZMB in Hamburg. Thanks go to all technicians who worked on the DZMB HH specimens for providing the data from the sorting process (DZMB database). Maksymilian Prondzynski spent a lot of energy taking the SEM pictures during a practical course in 2011. Karen Jeskulke is thanked for all her efforts in the laboratory of the University of Hamburg. Amy Driskell and Andrea Ormos supported us in the barcoding approach during our working visits at the Smithsonian after the DIVA-3 expedition. Financial support from CeDAMar for the 'DNA barcoding deep-sea Isopoda' project is highly appreciated. The curators of the AMNH (Marc Siddal) and USNM (Chad Walter) are thanked for providing type material. We would like to thank Ron Etter and his lab for looking for ethanol-fixed North Atlantic specimens from revisited Hessler stations. Two anonymous referees improved the quality of our article.

REFERENCES

Beddard FE. 1884. Report on the Isopoda collected by H.M.S. Challenger during the years 1873–76. Part I. – The genus *Serolis*. Report on the Scientific Results of the Voyage of H.M.S. Challenger during the years 1873–76. *Zoology* **11:** 1–85, pls I–X.

Bergsten J, Bilton DT, Fujisawa T, Elliott M, Monaghan MT, Balke M, Vogler AP. 2012. The effect of geographical scale of sampling on DNA barcoding. *Systematic Biology* **61:** 851–869.

Bonnier J. 1896. Édriophthalmes. *Ann. Univ. Lyon* 1895, 527–689.

Brandt A. 1988. *Antarctic Serolidae and Cirolanidae (Crustacea, Isopoda): new genera, new species, and redescriptions, with a key to the Antarctic Serolidae and Cirolanidae*. Königstein: Koeltz, Theses Zoologicae, 143 pages.

Brandt A. 1991. Zur Besiedlungsgeschichte des antarktischen Schelfes am Beispiel der Isopoda (Crustacea, Malacostraca). *Berichte zur Polarforschung* **98:** 1–240.

Brandt A. 1992. Origin of Antarctic Isopoda (Crustacea, Malacostraca). *Marine Biology* **113:** 415–423.

Brandt A. 2009. *Acutiserolis poorei* sp. nov. from the Amundsen Sea, Southern Ocean (Crustacea, Isopoda, Serolidae). *Memoirs of the Museum of Victoria, Australia* **66:** 17–24.

Brandt A, Brenke N, Andres HG, Brix S, Guerrero-Kommritz J, Mühlenhardt-Siegel U, Wägele JW. 2005. Diversity of peracarid crustaceans (Malacostraca) from the abyssal plain of the Angola Basin. *Organisms, Diversity & Evolution* **5:** 105–112.

Brandt A, Gooday AJ, Brix SB, Brökeland W, Cedhagen T, Choudhury M, Cornelius N, Danis B, De Mesel I, Diaz RJ, Gillan DC, Ebbe B, Howe J, Janussen D, Kaiser S, Linse K, Malyutina M, Brandao S, Pawlowski J, Raupach M. 2007. The Southern Ocean deep sea: first insights into biodiversity and biogeography. *Nature* **447:** 307–311.

Brandt A, Poore G. 2003. Higher classification of flabelliferan and related Isopoda based on a reappraisal of relationships. *Invertebrate Systmatics* **17:** 893–923.

Brix S, Leese F, Riehl T, Kihara TC. 2014. A new genus and new species of Desmosomati–dae Sars, 1897 (Isopoda) from the east South–Atlantic abyss described by means of integrative taxonomy. *Marine Biodiversity* doi:10.1007/s12526–014–0218–3.

Brix S, Savarsson J, Leese F. 2014. A multi-gene analysis reveals divergent lineages inside the isopod *Chelator insignis* (Hansen, 1916) South of Iceland. IceAGE special volume. *Polish Polar Research* **35:** 225–242.

Brix S, Riehl T, Leese F. 2011. First genetic data for species of the genus *Haploniscus* Richardson, 1908 (Isopoda: Asellota: Haploniscidae) from neighbouring deep-sea basins in the South Atlantic. *Zootaxa* **2838:** 79–84.

Brix S, Svavarsson J. 2010. Distribution and diversity of desmosomatid and nannoniscid isopods (Crustacea) on the Greenland–Iceland–Faeroe Ridge. *Polar Biology* **33:** 515–530.

Brökeland W. 2010. Description of four new species from the *Haploniscus unicornis* Menzies, 1956 complex (Isopoda: Asellota: Haploniscidae). *Zootaxa* **2536:** 1–35.

Brökeland W, Brandt A. 2004. Neoteny in the deep sea asellote family Ischnomesidae (Crustacea: Isopoda) and descriptions of two new species from the Southern Ocean. *Deep-Sea Research II* **51:** 1769–1787.

Bruce NL. 2009. New genera and species of the marine isopod family Serolidae (Crustacea, Sphaeromatidea) from the south-western Pacific. *ZooKeys* **18:** 17–76.

Buhay JE. 2009. 'COI-like' sequences are becoming problematic in molecular systematics and DNA bar-coding studies. *Journal of Crustacean Biology* **29:** 96–110.

Cals P. 1982. Spéciation de crustacés benthiques en fonction de l'évolution tectonique des fonds oceaniques. *Bulletin de la Société Géologique de France* **24:** 935–941.

Coleman CO. 2003. 'Digital inking': how to make perfect line drawings on computers. *Organisms, Diversity & Evolution* **3:** 303–304.

Costello M, May RM, Storck NE. 2013. Can we name earth's species before they go extinct? *Science* **339:** 413–416.

Dana JD. 1853. Crustacea Edriophthalmia. *United States Exploring Expedition during the years 1838, 1839, 1840, 1841, 1842 under the command of Charles Wilkes, U.S.N.* 13(2): 695–797.

Folmer O, Black M, Hoeh W, Lutz R, Vrijenhoek R. 1994. DNA primers for amplification of mitochondrial cytochrome c oxidase subunit I from diverse metazoan invertebrates. *Molecular Marine Biology and Biotechnology* **3:** 294–299.

George RY. 1986. *Serolis agassizi*, new species, from the deep sea off Cape Fear, north Carolina (Crustacea: Isopoda). *Proceedings of the Biological Society of Washington* **99:** 46–50.

Grassle JF, Maciolek N. 1992. Deep-sea species richness: regional and local diversity estimates from quantitative bottom samples. *American Naturalist* **139:** 313–341.

Harrison K, Poore GCB. 1984. *Serolis* (Crustacea, Isopoda, Serolidae) from Australia with a new species from Victoria. *Memoirs of the Museum of Victoria* **45:** 13–31.

Held C. 2000. Phylogeny and biogeography of serolid isopods (Crustacea, Isopoda, Serolidae) and the use of ribosomal expansion segments in molecular systematics. *Molecular Phylogenetics and Evolution* **15:** 165–178.

Held C. 2003. Molecular evidence of cryptic speciation within widespread Antarctic crustcean Ceratoserolis trilobitoides (Crustacea, Isopoda). *Antarctic Biology in a Global Centext*: 135–139.

Held C, Wägele JW. 2005. Cryptic speciation in the giant Antarctic isopod Glyptonotus antarcticus (Isopoda: Valvifera: Chaetiliidae). *Scientia Marina* **69:** 175–181.

Hessler RR. 1967. A record of Serolidae (Isopoda) from the North Atlantic Ocean. *Crustaceana* **12:** 159–162.

Hessler RR. 1969. Peracarida Isopoda. In: Moore RC, ed. *Treatise on Invertebrate Palaeontology*. New York: Geological Society America, R371–R384.

Hessler RR. 1970. A new species of Serolidae (Isopoda) from bathyal depths of the equatorial Atlantic Ocean. *Crustaceana* **18:** 227–232.

Hogg NG, Owens WB, Siedler G, Zenk W. 1996. Circulation in the deep Brazil basin. In: Wefer G, Berger WH, Siedler G, Webb DJ, eds. *The South Atlantic: present and past circulation*. Berlin, Heidelberg: Springer-Verlag, 249–260.

Janosik AM, Halanych KM. 2010. Unrecognized Antarctic biodiversity: a case study of the genus *Odontaster* (Odontasteridae; Asteroidea). *Integrative and Comparative Biology* **50:** 981–992.

Kihara T, Da Rocha C. 2009. *Técnicas para o estudo taxonomico de copépodes harpacticóides da meiofauna marinha*. Porto Alegre: Asterisco.

Kröncke I, Reiss H, Türkay M. 2013. Macro- and megafauna communities in three deep basins of the South-East Atlantic. *Deep-Sea Research 1* **81:** 25–35.

Leese F, Agrawal S, Held C. 2010. Long-distance island hopping without dispersal stages: transportation across major zoogeographic barriers in a Southern Ocean isopod. *Die Naturwissenschaften* **97:** 583–594.

Leese F, Held C. 2008. Identification and characterization of microsatellites from the Antarctic isopod *Ceratoserolis trilobitoides*: nuclear evidence for cryptic species. *Conservation Genetics* **9:** 1369–1372.

Leese F, Kop A, Wägele JW, Held C. 2008. Cryptic speciation in a benthic isopod from Patagonian and Falkland Island waters and the impact of glaciations on its population structzure. *Frontiers in Zoology* **5:** 19–34.

Lefebure T, Douday CJ, Gouy M, Tontelj P, Briolay J, Gibert J. 2006. Phylogeography of a subterranean amphipod reveals cryptic diversity and dynamic evolution in extreme environments. *Molecular Ecology* **15:** 1797–1806.

Maddison WP, Maddison DR. 2011. *Mesquite: a modular system for evolutionary analysis. Version 2.75*. Available at: http://mesquiteproject.org

Menzies RJ. 1962. The isopods of abyssal depths in the Atlantic Ocean. *Abyssal Crustacea* **1:** 79–206.

Michels J, Büntzow M. 2010. Assessment of Congo red as a fluorescence marker for the exoskeleton of small crustaceans and the cuticle of polychaetes. *Journal of Microscopy* **238:** 95–101.

Miers EJ. 1881. On a collection of Crustacea made by Baron Hermann-Maltzan at Goree Island, Senegambia. *Annals and Magazine of Natural History* **8:** 364–377.

Moreira PS. 1977. Crustacea Isopoda collected during the OC/S 'Almirante Saldanha' cruises in Southern South America, II.

Additions to the species of *Serolis* (Flabellifera, Serolidae). *Boletim do Instituto Oceanográfico*, Sãn Paulo **26,** 257–271.

Palumbi SR, Benzie J. 1991. Large mitochondrial DNA differences between morphologically similar Penaeid shrimps. *Molecular Marine Biology and Biotechnology* **1:** 27–34.

Passamonti M, Ghiselli F. 2009. Doubly uniparental inheritance: two mitochondrial genomes, one precious model for organelle DNA inheritance and evolution. *DNA and Cell Biology* **28:** 79–89.

Poore GCB. 1984. *Colanthura, Califanthura, Cruranthura* and *Cruregens* related genera of the Paranthuridae. *Journal of Natural History* **18:** 697–715.

Poore GCB. 1985. *Basserolis kimblae*, a new genus and species of isopod (Serolidae) from Australia. *Journal of Crustacean Biology* **5:** 175–181.

Poore GCB. 1987. *Serolina*, a new genus for *Serolis minuta* Beddard (Crustacea: Isopoda: Serolidae) with descriptions of eight new species from Australia. *Memoirs of the National Museum of Victoria* **48:** 141–189.

Poore GCB. 1990. Two new species of isopod crustaceans belonging to Australian endemic genera (Serolidae and Chaetiliidae). *Memoirs of the Museum of Victoria* **51:** 99–107.

Poore GCB, Brandt A. 1997. Crustacea Isopoda Serolidae: *Acutiserolis cidaris* and *Caecoserolis novaecaledoniae*, two new species from the Coral Sea. Res. Camp. Musorstom 18. *Memoirs of the Museum of Natural History* **176:** 151–168.

Poore GCB, Bruce N. 2012. Global diversity of marine isopods (except Asellota and crustaceans symbionts). *PLoS ONE* **7:** 1–15.

Poore GCB, Storey JM. 2009. *Brucerolis*, new genus, and *Acutiserolis* Brandt, 1988, deep-water southern genera of isopods (Crustacea, Isopoda, Serolidae). *ZooKeys* **129:** 1–14.

Posada D, Buckley TR. 2004. Model selection and model averaging in phylogenetics: advantages of akaike information criterion and bayesian approaches over likelihood ratio tests. *Systematic Biology* **53:** 793–808.

Raupach M, Wägele J-W. 2006. Distinguishing cryptic species in Antarctic Asellota (Crustacea: Isopoda) – a preliminary study of mitochondrial DNA in *Acanthaspidia drygalskii*. *Antarctic Science* **18:** 191–198.

Reid JR. 1996. On the circulation of the South Atlantic Ocean. In: Wefer G, Berger WH, Siedler G, Webb DJ, eds. *The South Atlantic: present and past circulation*. Berlin, Heidelberg: Springer-Verlag, 13–44.

Rex MA, Stuart CT, Hessler RR, Allen JA, Sanders HL, Wilson GDF. 1993. Global-scale latitudinal patterns of species diversity in the deep-sea benthos. *Nature* **365:** 636–639.

Rex MA, McClain CR, Johnson NA, Etter RJ, Allen JA, Bouchet P, Warén A. 2005a. A source-sink hypothesis for abyssal biodiversity. *The Americal Naturalist* **165:** 163–178.

Rex MA, Crame A, Stuart CT, Clarke A. 2005b. Large-scale biogeographc patterns in marine molluscs: a confluence of history and productivity? *Ecology* **86:** 2288–2297.

Riehl T, Brandt A. 2010. Two new species in the genus *Macrostylis* Sars, 1964 (Isopoda, Asellota, Macrostylidae) from the Weddell Sea, with a synonymisation of *Desmostylis* Brandt, 1992 with *Macrostylis*. *Zookeys* **57:** 9–49.

Riehl T, Kaiser S. 2012. Conquered from the deep sea? A new deep-sea isopod species from the Antarctic shelf shows pattern of recent colonization. *PLoS ONE* **7:** e49354.

Sanders HL, Hessler RR. 1969. Diversity and composition of abyssal benthos. *Science* **166:** 1033–1034.

Schnurr S, Brandt A, Brix S, Fiorentino D, Svavarsson J. 2013. Composition and distribution of selected munnopsid genera (Crustacea, Isopoda, Asellota) in Icelandic waters. *Deep Sea Research Part I* **84:** 42–155.

Schotte M, Kensley B, Shilling S. 1995 onwards. *World list of marine, freshwater and terrestrial Crustacea Isopoda*. National Museum of Natural History Smithsonian Institution: Washington D.C., USA. Available at: http://wwwnmnhsiedu/iz/isopod/

Sheppard EM. 1933. Isopoda Crustacea Part I. The family Serolidae. *Discovery Reports* **7:** 253–362.

Storey MJ, Poore GCB. 2009. New species of *Brucerolis* (Crustacea: Isopoda: Serolidae) from seas around New Zealand and Australia. *Memoirs of Museum Victoria* **66:** 147–173.

Suhm WR. 1874. Von der Challenger-Expedition. Briefe an C. Th. E. von Siebold. II. *Zeitschrift für Wissenschaftliche Zoologie* **24:** IX–XXIII.

Tattersall WM. 1905. The marine fauna of the coast of Ireland. Part V. Isopoda. *Reports of the Department of Agriculture and Technical Instruction for Ireland, Scientific Investigations of the Fisheries Branch, 1904* 2: 53–142.

Teske PR, McQuaid CD, Froneman PW, Barker NP. 2006. Impacts of marine biogeographic boundaries on phylogeographic patterns of three South African estuarine crustaceans. *Marine Ecology Progress Series* **314:** 283–293.

Thistle D. 2003. The deep-sea floor: an overview. In: Tyler PA, ed. *Ecosystems of the World 28*. Amsterdam, The Netherlands: Elsevier Science, 5–37.

Vincx M, Bett BJ, Dinet A, Ferrero T, Gooday AJ, Lambshead PJD, Pfannkuche O, Soltwedel T, Vanreusel A. 1994. Meiobenthos of the deep northeast Atlantic: a review. *Advances in Marine Biology* **30:** 1–88.

Wägele JW. 1989. Evolution und phylogenetisches System der Isopoda. Stand der Forschung und neue Erkenntnisse. *Zoologica* **140:** 1–262.

Wägele JW. 1994. Notes on Antarctic and South American Serolidae (Crustacea, Isopoda) with remarks on the phylogenetic biogeography and a description of new genera. *Zoologische Jahrbücher. Abteilung für Systematik* **121:** 3–69.

Webb DJ. 1996. The southern boundary of the South Atlantic. In: Wefer G, Berger WH, Siedler G, Webb DJ, eds. *The South Atlantic: present and past circulation*. Berlin, Heidelberg: Springer-Verlag, 211–217.

Wefer G, Berger WH, Siedler G, Webb DJ, eds. 1996. *The South Atlantic: present and past circulation*. Berlin, Heidelberg: Springer-Verlag, 1–644.

Wetzer R, Pérez-Losada M, Bruce NL. 2013. Phylogenetic relationships of the family Sphaeromatidae Latreille, 1825 (Crustacea: Peracarida: Isopoda) within Sphaeromatidea based on 18S-rDNA molecular data. *Zootaxa* **3599:** 161–177.

Wolff T. 1962. The systematics and biology of bathyal and abyssal Isopoda Asellota. *Galathea Report* **6:** 1–320.